Tuning Electronic States of a CdSe/ZnS Quantum Dot by Only One Functional Dye Molecule

Eduard Zenkevich,[†] Aleksander Stupak,[‡] Clemens Göhler,[§] Cornelius Krasselt,[§] and Christian von Borczyskowski*[,§]

[†]Department of Information Technologies and Robotics, National Technical University of Belarus, Nezavisimosti Ave., 65, 220013 Minsk, Belarus, [‡]B.I. Stepanov Institute of Physics, National Academy of Science of Belarus, Nezavisimosti Ave., 70, 220072 Minsk, Belarus, and [§]Institute of Physics, Technische Universität Chemnitz, Reichenhainerstr. 70, 09107 Chemnitz, Germany

ABSTRACT Self-assembly of only one functionalized porphyrin dye molecule with one CdSe/ZnS quantum dot (QD) not only modifies the photoluminescence (PL) intensity but also creates a few energetically clearly distinguishable electronic states, opening additional effective relaxation pathways. The related energy modifications are in the range of 10−30 meV and show a pronounced sensitivity to the specific nature of the respective dye. We assign the emerging energies to surface states. Time-resolved PL spectroscopy in combination with spectral deconvolution reveals that surface properties of QDs are a complex interplay of the nature of the dye molecule and the topography of the ligand layer across a temperature range from 77 to 290 K. This includes a kind of phase transition of trioctylphosphine oxide ligands, switching the nature of surface states observed below and above the phase transition temperature. Most importantly, our findings can be closely related to recent calculations of ligand-induced modifications of surface states of QDs. The identification of the optical properties emerged from a combination of spectroscopy on single QDs and QDs in an ensemble.

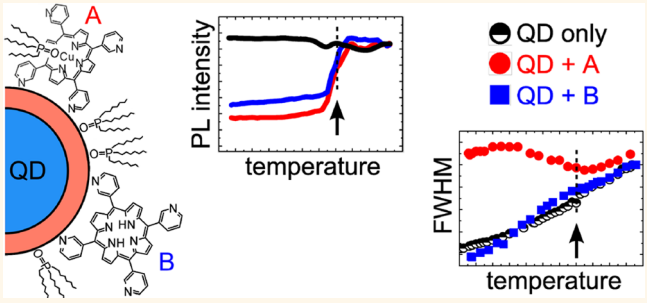

KEYWORDS: quantum dot/dye nanoassemblies · photoluminescence intermittency · single quantum dots · spectral diffusion · photoluminescence decay · CdSe/ZnS · photoluminescence spectra · pyridyl-substituted porphyrins · temperature dependence · ligands

Science and technology of nanoparticle-based materials, such as semiconductor quantum dots (QDs), involve surface and interfacial phenomena that may be tuned by tailoring the surface state energy and by varying the specific electronic interactions with chemical entities attached to such surfaces and interfaces.[1] The main obstacle on the path to develop efficient QD-based energy materials is our limited understanding of QD surfaces, their interaction with surface-ligated molecules, and their impact on charge or energy transfer between QDs and attached molecules. Optical properties might be tuned specifically *via* the interaction of semiconductor nanoparticles with functional organic molecules. Of special interest is the basic understanding of a one-molecule-to-one-QD base. If successfully applied, the large variety of functional organic molecules at hand allows for a broad scenario for modification of optical QD properties.[2−4]

One well-established class of nanomaterials is based on colloidal core/shell QDs. Capping organic shells (including surfactants and ligands) have considerable impact on the optical properties of QDs, as has been successfully studied experimentally and theoretically for several systems.[5−10] Several experiments demonstrate the influence of ligand shells on surface structure,[11] hot carrier relaxation,[12] quantum yield,[12,13] and photoluminescence (PL) energy.[9,14] However, detailed and specific experimental studies on the influence of only one (or at least a few) ligand or surface-attached dye molecules on surface states are difficult to conceive. To the best of our knowledge, related studies have not yet been reported. Fortunately, recent progress in calculations of the structures and electronic properties[15−20]

* Address correspondence to borczyskowski@physik.tu-chemnitz.de.

Received for review December 5, 2014 and accepted February 21, 2015.

Published online February 22, 2015
10.1021/nn506941c

has set new milestones in the understanding QD surfaces and the impact of ligands and solvents. Calculations show that ligands cause (depending on their concrete number) surface reconstruction; they modify, even on a single ligand base, electronic states or electron−phonon coupling and hot carrier relaxation.[21−24] Pronounced dependencies on structure-related specific positions of surface atoms have also been identified,[23] including the mobility of individual surface atoms or ligands.[25−28]

Now it is a challenge for experimentalists to reach on a single ligand (or dye) level a comparable sophistication of QD surface characterization in order to finally tailor electronic properties on demand. We attempt to close this gap between calculations and experiment on the level of a single molecule. Our approach is based on the replacement of one or at most a few ligands by exactly one organic dye molecule because a dye allows, as a kind of spectator, an efficient and direct optical access.

There are ample investigations on nanoassemblies formed by one or a few functionalized dye molecules attached to a QD surface, which mostly report the influence of the attached dye upon the PL intensity of II/VI colloidal QDs.[14,29−34] However, a microscopic understanding of the interaction with the QD surface is far from being at hand. The present publication aims as a first approach to elucidate such QD−dye interactions with respect to PL intensity changes and, more specifically, to the fine-tuning of electronic states at the surface of CdSe/ZnS QDs. Dye-induced surface states have been predicted in recent calculations.[21] Since dye molecules replace ligands,[35,36] we will discuss experimental results with respect to the replacement of a few ligands by only one dye molecule.

We will make use of the concept of the self-assembly of QDs and functionalized porphyrins[30,34,36−38] or other molecules previously reported by us[33,35,39] and others.[29,31,32,40−42] We have chosen porphyrins because their attachment to the QD surface has uniquely been identified for many porphyrins of trioctylphosphine oxide (TOPO)-capped QDs of various sizes.[30,36,37] Moreover, porphyrins allow, due to their intrinsic nature, for a wide range of functionalization (*via* the number and positions of functional groups) and modification of the central ion.[30,37]

To approach the goal of identifying specific electronic surface interactions, we present (temperature-dependent) spectroscopic and time-resolved PL experiments on CdSe/ZnS QD−porphyrin nanoassemblies in an ensemble. Though we make use of conventional PL spectroscopy, we are nevertheless sensitive to the chemical nature of the respective porphyrin molecules and the impact of the competing ligand layer.

The interpretation of such an elaborate investigation on an ensemble of nanoassemblies becomes only feasible upon comparison with results obtained by a newly designed and complementary (time and spectrally resolved) spectroscopy on single QDs. These experiments establish a link between the (heterogeneous) ensemble and single QDs, including blinking and spectral diffusion phenomena.[43−45] Though weak ergodicity breaking has been reported in the case of (blinking) single QDs,[46,47] a comparison between spectroscopic data of single and ensemble data shows basically a close relationship between both kinds of experimental approaches.

In the majority of reports on QD−dye nanoassemblies, the observed PL quenching for the QD component has been assigned to Förster resonance energy transfer (FRET), which is in many cases is only half of the truth since PL quenching might be related to non-FRET processes, as we have recently shown qualitatively.[35−37,48] In the present paper, we report quantitatively the reasons for such non-FRET quenching processes.

We will report that one dye molecules replaces (a few) ligand molecules, which results in PL energy shifts of 10−30 meV and in increased nonradiative relaxation pathways causing QD PL quenching. The experimental findings will supplement recent calculations on detailed surface properties.[16−18,20−22]

RESULTS

Ensemble Experiments. We have shown earlier that *meso*-pyridyl-functionalized porphyrins form nanoassemblies with CdSe/ZnS or CdSe and quench the PL of QDs[30−42] caused by attachment to the QD surface *via* their *meso*-pyridyl groups (see Scheme 1).[30,34,36−38] At a molar concentration ratio of $[C_{Dye}]/[C_{QD}] = x = 1$, not all porphyrin molecules are attached to the QD surface because of dynamic equilibrium conditions.[36] Since the influence of assembly formation on QD PL spectra has not yet been reported at very low dye concentrations, we now investigate the PL spectra of CdSe/ZnS nanoassemblies with *meso*-pyridyl porphyrins in a glassy matrix between 77 and 290 K.

Figure 1 shows normalized PL spectra of CdSe/ZnS as part of H_2P-CdSe/ZnS (2) or CuP-CdSe/ZnS (3) nanoassemblies in comparison to those for CdSe/ZnS QDs (1) at high and low temperatures. Spectra of CdSe/ZnS and QDs in nanoassemblies are very similar but not identical at 288 or 290 K, respectively.

The situation is markedly different at 95 K, as can be seen from Figure 1. PL spectra of all types of QDs are shifted to the blue (and narrowed in spectral width) upon temperature decrease, which is due to decreased electron−phonon coupling.[49−54] When PL bands of CdSe/ZnS (1) at 95 K are compared with those of QDs in nanoassemblies, an additional small blue shift is observed in the case of H_2P-CdSe/ZnS (2) (Figure 1A), while the PL band is more strongly blue-shifted and considerably broadened for QDs in CuP-CdSe/ZnS (3) nanoassemblies (Figure 1B). These observations are

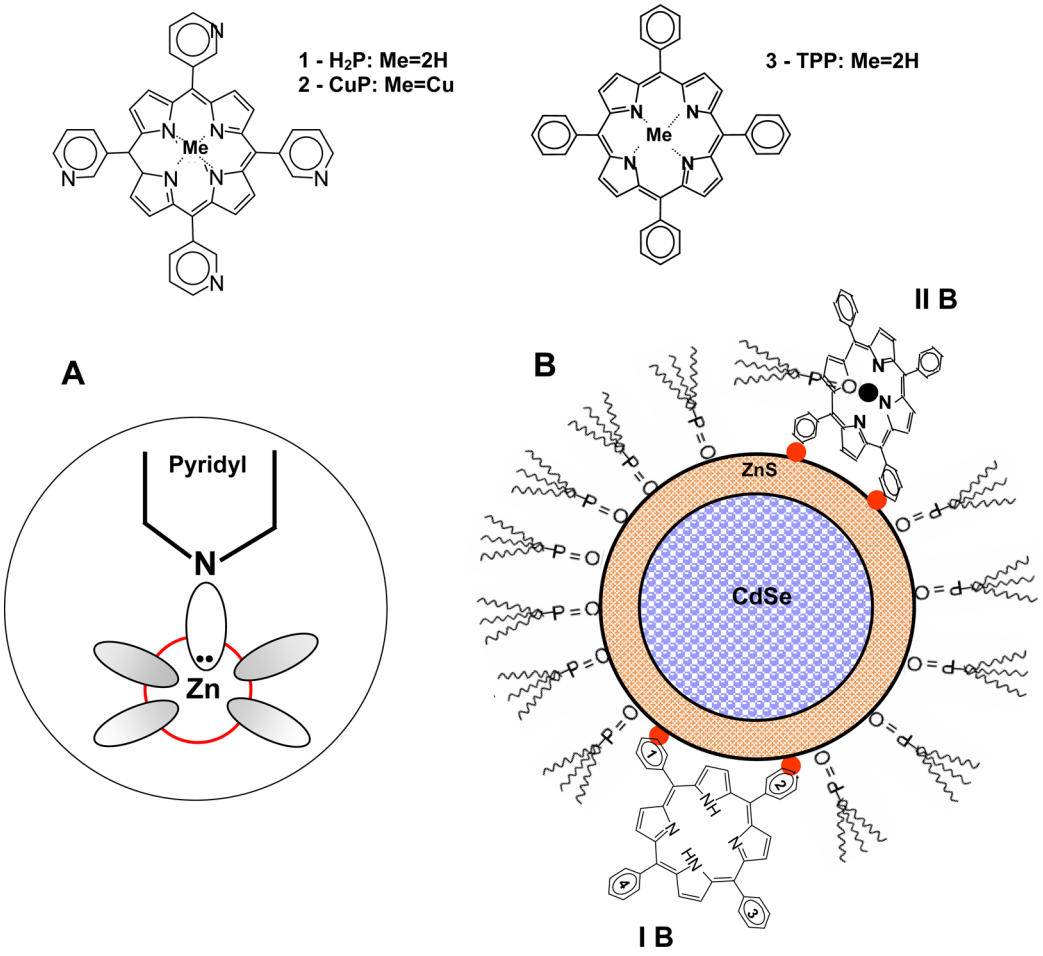

Scheme 1. Chemical structures of 5,10,15,20-*meso*-*meta*-pyridyl porphyrins [free base (H_2P, 1), Cu complex (CuP, 2), and *tetra*-phenylporphyrin (TPP, 3)]. Scheme for the coordination of porphyrins to the ZnS shell *via* pyridyl N···Zn interaction (A) as well as schematic presentation of the mutual arrangement of a porphyrin molecule with respect to the QD surface (B). Nitrogen lone pair orbitals (participating in Zn−N coordination) are indicated by a red dot. Capping ligands, TOPO, are depicted also. I B shows coordination of H_2P and CuP porphyrins on the QD surface, while II B shows additional extra ligation of a TOPO molecule to the central Cu atom of the CuP molecule (see explanation in the text).

quite remarkable because they are caused, on average, by at most one porphyrin molecule per QD.

We show in Figure 2A the temperature dependence of the PL intensity for all three entities depicted in Figure 1. To remove the intrinsic temperature effects caused by electron−phonon coupling, we show in Figure 2B the temperature-dependent but normalized integrated PL intensities for QDs in nanoassemblies relative to the PL intensity of CdSe/ZnS. Curve 1 in Figure 2B presents the temperature dependence of the ratio of the PL for QDs in the presence of, but not complexed with, *tetra*-phenylporphyrin (TPP) molecules (not having functional *meso*-pyridyl rings; see Scheme 1).[30,36] The ratio is within 5% constant over the total temperature range.

In contrast, for PL of QDs in H_2P-CdSe/ZnS or CuP-CdSe/ZnS nanoassemblies, we observe a sudden change of the PL ratio close to $T_{crit} \approx 220$ K (curves 2 and 3), which can be interpreted as a sudden change of porphyrin induced PL quenching. Moreover, PL quenching of QDs below T_{crit} is stronger for CuP-CdSe/ZnS compared to H_2P-CdSe/ZnS nanoassemblies. A temperature T_{crit} has been recently identified to be a signature of a "phase transition" of the ligand shell of CdSe QDs being initially dissolved in liquid solution at ambient temperature.[55,56] A strong PL intensity jump has not been reported for CdSe/ZnS,[57] but present experiments show a weak intensity jump also for CdSe/ZnS (see curve 1 in Figure 2A), which is obviously strongly increased upon attachment of one porphyrin molecule (curves 2 and 3).

Figure 2 shows the energy, E_{max}, of the PL band maximum (Figure 2C) and the spectral line width fwhm (Figure 2D) obtained by fitting to a Gaussian line shape. According to electron−phonon coupling models, E_{max} should shift to lower energies and fwhm should increase.[51−54] As expected, we observe in all cases a continuous shift to low energies upon increasing temperature, which is superimposed by a sudden jump to higher energies at $T_{crit} \approx 220$ K (Figure 2C). Additionally, there are noticeable variations in the temperature dependence of the different nanoassemblies.

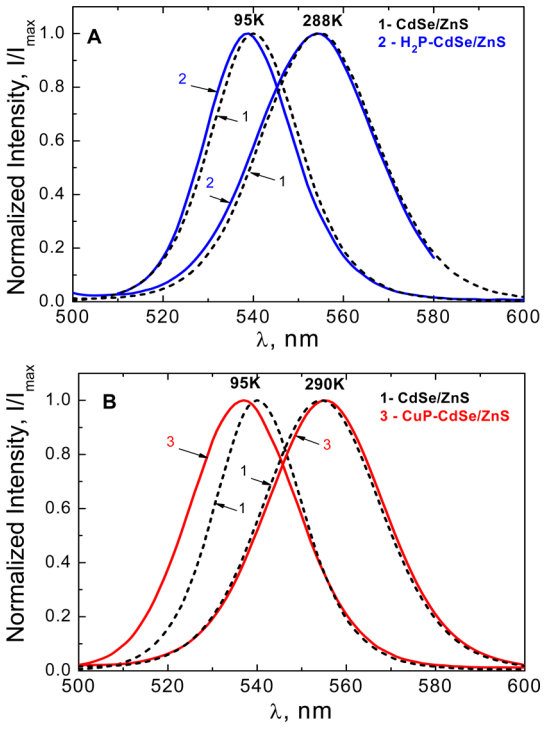

Figure 1. Normalized PL spectra of CdSe/ZnS QDs (1, broken line) and QDs (A) in H_2P-CdSe/ZnS (2) and (B) CuP-CdSe/ZnS (3) nanoassemblies at a molar ratio of x = 1 in a methylcyclohexane/toluene (6:1) mixture at ambient (288−290 K) and low (95 K) temperature for excitation at λ_{exc} = 450 nm. The corresponding PL band maxima, λ_{max}, are as follows: 288−290 K, 555 nm (1), 554 nm (2), and 556 nm (3); 95 K, 540 nm (1), 539 nm (2), and 537 nm (3). Notably, the observed blue shift of QD PL at 95 K is not due to a size selection *via* excitation. In the given case, all QDs have been excited into high excitonic states (at λ_{exc} = 450 nm), thus excluding size selection.[38]

The comparison of the spectral widths in Figure 2D reveals that fwhm values increase—but noticeably different for each entity—with increasing temperature for CdSe/ZnS and QDs in H_2P-CdSe/ZnS nanoassemblies. However, for the fwhm of QD PL in CuP-CdSe/ZnS nanoassemblies, we find an only moderate temperature-dependent (broad) line across the temperature range, which is not typical for electron−phonon coupling. We like to emphasize again that this finding is caused, on average, by only one CuP molecule.

Supplementing investigations of temperature-dependent PL properties of CdSe/ZnS and QDs in CuP-CdSe/ZnS nanoassemblies deposited onto a quartz glass substrate (for which TOPO and porphyrin exchange dynamics are definitely excluded) reveal a very similar behavior with respect to PL spectral and decay components as in the glass-forming solvent (see Supporting Information, Figures S3 and S4). This finding confirms that PL properties are significantly modified upon assembly formation, independent of the embedding matrix.

All of these variations of PL parameters prompt us to postulate the presence of several assembly-dependent spectral components constituting a PL band. In particular, the strong fwhm broadening and energy shift of the QD PL in CuP-CdSe/ZnS assemblies (see Figures 1B and 2D) strongly support a spectral deconvolution into at least two spectral components. In fact, an improved approximation of the band shape is achieved by assuming at least two Gaussian PL components. Figure 3 shows as a function of temperature (A) the maximum $(E_{max})_i$, (B) the related spectral line width $(fwhm)_i$, and (C) the integrated intensity I_i for the two spectral components obtained for CdSe/ZnS QDs (left) and CdSe/ZnS in H_2P-CdSe/ZnS (middle) or in CuP-CdSe/ZnS (right). In all cases, we find a broad (B) and a narrow (N) spectral component. In Figure 3D, we plot the ratio of PL intensities of the narrow band N to the broad band B. It is quite remarkable that all temperature dependencies differ strongly among each other. We will evaluate the statistical relevance of the fitting procedure in the Discussion section.

The energy difference ΔE between the B and N band component varies by only a few millielectronvolts for CdSe/ZnS over the temperature range. Above $T_{crit} \approx$ 220 K, $(E_{max})_i$ values are nearly identical. Deviations from a continuous change with temperature are observed in the vicinity of $T_{crit} \approx$ 220 K, which becomes most obvious when inspecting the PL intensity ratio in Figure 3D.

For the emission of QDs in H_2P-CdSe/ZnS nanoassemblies, we observe an increase of ΔE and a large change of relative intensities (Figure 3D) while the temperature dependence of $(E_{max})_i$ and $(fwhm)_i$ is similar to the one obtained for CdSe/ZnS. Assignment of PL energies according to the spectral widths N and B crossing of energies is observed at T_{crit} (Figure 3A).

The situation is much more complex for QDs in CuP-CdSe/ZnS nanoassemblies. While the energy variation of the broad component B is similar to the one of CdSe/ZnS QDs, the corresponding variation of the narrow component N deviates from the corresponding one of QDs in H_2P-CdSe/ZnS. We observe, in addition to a jump of energies at T_{crit}, an apparent crossing of energies at $T \approx$ 130 K.

The separation of PL energies is larger for QDs in nanoassemblies as compared to CdSe/ZnS. A remarkable finding is that at low temperatures the energy separation ΔE between the B and N component increases from CdSe/ZnS to QDs in H_2P-CdSe/ZnS and further to CuP-CdSe/ZnS nanoassemblies. Close to 130 K, deconvolution into two PL bands was difficult to realize for QDs in CuP-CdSe/ZnS nanoassemblies due to the apparent crossing of bands N and B. There are probably more than two spectral components, which all depend differently on temperature, resulting in this case in a noncontinuous behavior at $T \approx$ 130 K. However, the identification of more than two spectral components is beyond our experimental accuracy. Nevertheless, a safe conclusion is that a narrow component N emerges for CuP-CdSe/ZnS, which is

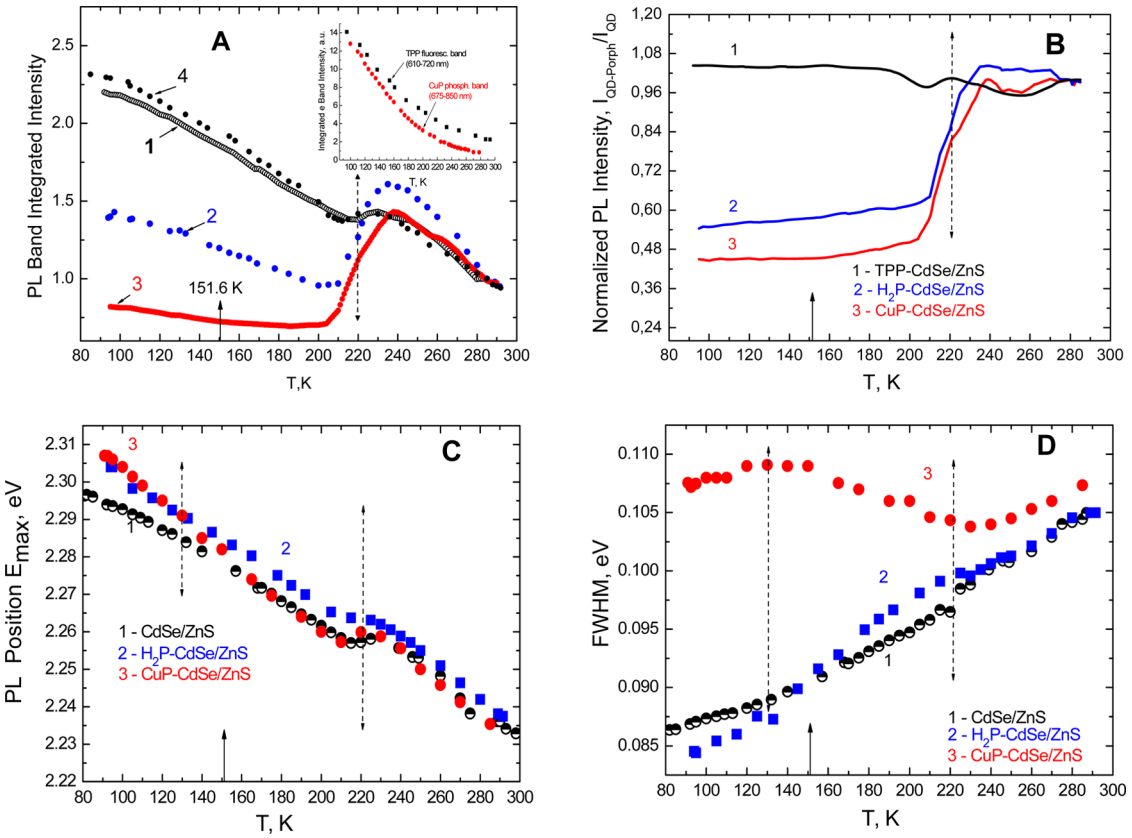

Figure 2. Temperature dependence of (A) QD PL band integrated intensities, (B) normalized QD PL intensity ratio, (C) PL band energy position, and (D) full width at half-maximum (fwhm) for TOPO-capped CdSe/ZnS (1) and for QDs in H_2P-CdSe/ZnS (2) and CuP-CdSe/ZnS (3) nanoassemblies at a molar ratio of $x = 1$ in a methylcyclohexane/toluene (6:1) mixture for $\lambda_{exc} = 450$ nm. Two temperatures, $T \approx 130$ K (see text) and $T_{crit} \approx 220$ K (phase transition assigned to the capping TOPO layer), are indicated by dashed arrows. The temperature of the glass transition for the methylcyclohexane/toluene (6:1) mixture at 151.6 K[84,85] is shown by an arrow (solid line). (A) (1) CdSe/ZnS QDs; nanoassemblies (2) H_2P-CdSe/ZnS, (3) CuP-CdSe/ZnS, and noncomplexed (4) TPP in a mixture with CdSe/ZnS.[50] All curves are normalized to 1 at 293 K. Relative intensities ($x = 1$; 293 K) are $I_1 = 1.0$ for CdSe/ZnS, $I_2 = 0.85$ for H_2P-CdSe/ZnS, $I_3 = 0.84$ for CuP-CdSe/ZnS, and $I_4 = 1.0$ for TPP-CdSe/ZnS. The inset shows, without the evidence of a phase transition, the temperature dependence for TPP fluorescence (black squares) and CuP phosphorescence (red dots) measured at the same conditions as for QD detection. (B) PL intensity ratios for (1) TPP-CdSe/ZnS, (2) H_2P-CdSe/ZnS, and (3) CuP-CdSe/ZnS normalized to the PL intensity of CdSe/ZnS. All ratios have been additionally normalized to 1 at $T = 280$ K. All intensity ratios have been normalized to 1 at 280 K to avoid the influence of varying initial conditions, such as absolute concentrations or (unidentified) PL quenching processes.

20 meV above the energies of QDs in H_2P-CdSe/ZnS nanoassemblies and which depends much stronger on temperature than the broad component B.

Additional information indicating energetic inhomogeneities stems from time-resolved PL data obtained at 77 and 290 K for various detection wavelengths across the PL bands of QDs. Details of the experimental findings of a three-exponential fit of the PL decay are shown in the Supporting Information (Figure S1). Table 1 summarizes all fitting parameters at two PL energies, namely, those at the respective high and low fwhm position of the total PL line width. In general, at low temperatures, PL decay times decrease with PL energy (see Figure S1 and Scheme S1).

Table 1 shows that both the absolute decay times τ_i and their relation to the spectral range depend noticeably on the kind of nanoassembly, which is in accordance with the observation that the composition of PL spectra depends strongly on the kind of nanoassembly (Figure 3). In addition, at both temperatures, the decrease of decay times upon nanoassembly formation reflects the presence of quenching processes for QD PL following attachment of only one porphyrin molecule, as was found by us earlier in titration experiments.[30,34,37] Usually, electron−phonon coupling will result in faster relaxation processes upon temperature increase. However, the opposite temperature dependence is observed by inspecting Table 1. This is a clear indication that the nature of PL states is different below and above T_{crit}.

Single QD Experiments. Ensemble experiments on QDs are hampered by the fact that it is not immediately obvious whether an identified variation of parameters (such as PL energies or decay times) is related to a distribution of QDs with different properties (ensemble average) or, alternatively, whether each QD explores these parameters in the course of the observation time (time average). To give more insight into this open

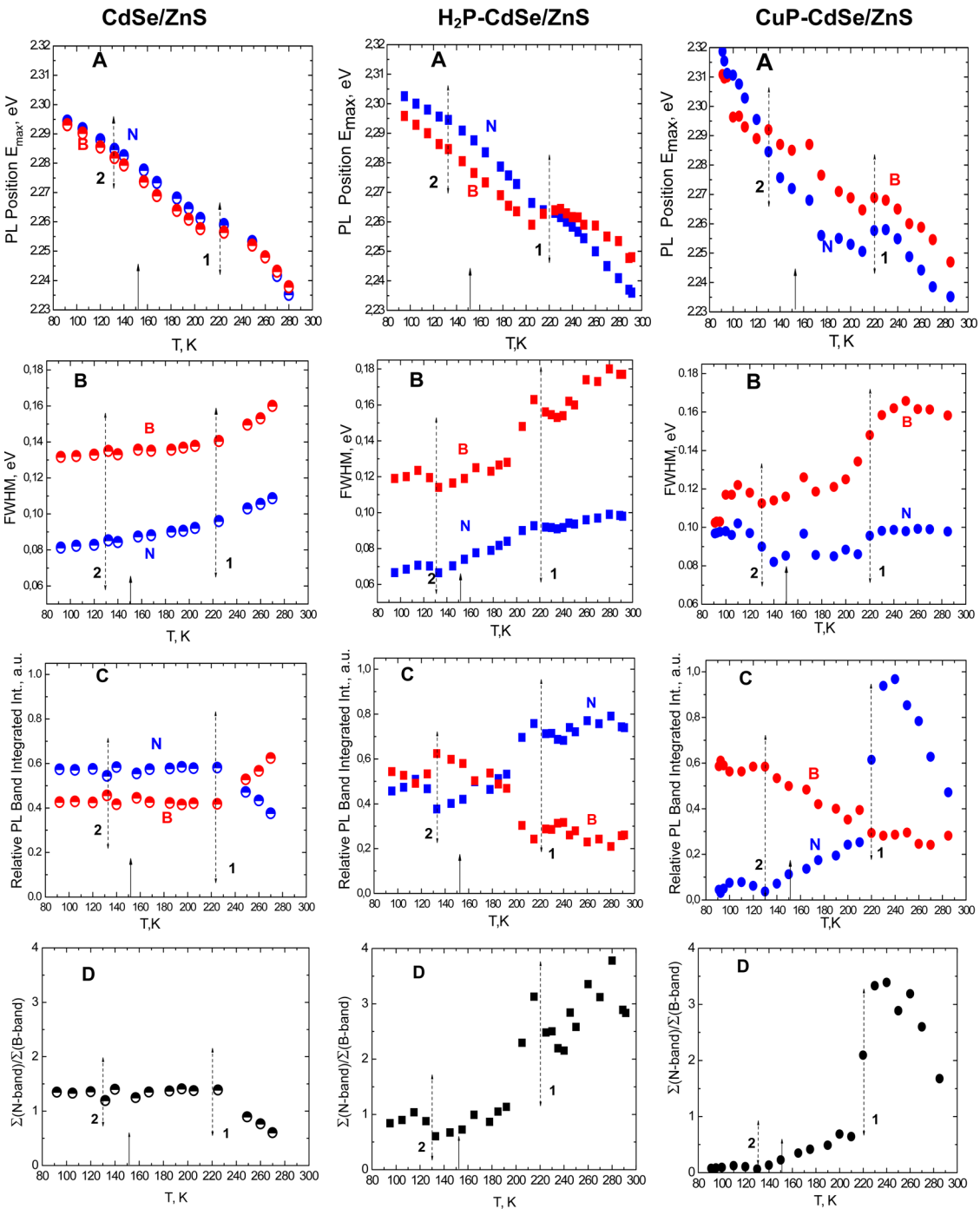

Figure 3. Temperature dependence of PL properties for (left) CdSe/ZnS QDs and for QDs in (middle) H_2P-CdSe/ZnS or (right) CuP-CdSe/ZnS nanoassemblies in a methylcyclohexane/toluene (6:1) mixture at λ_{exc} = 450 nm. (Fits have been obtained by two Gaussian components, termed B (broad) and N (narrow).) The temperature T_{crit} (≈220 K) of a phase transition of the capping TOPO layer is indicated by the dashed arrow (1). An additional discontinuity of some of the observables is found at $T \approx$ 130 K (indicated by the dashed arrow (2)). The glass transition temperatures of the components of the matrix are 146.7 K for methylcyclohexane, 180 K for toluene,[84] and 151.6 K for a methylcyclohexane/toluene (6:1) mixture.[84,85] The last temperature is shown by an arrow (solid line). (A) PL band energies, E_{max}, for N and B components. (B) Full spectral widths at half-maximum for N and B components. (C) Relative integrated PL band intensities for N and B components. (D) Ratio of integrated PL band intensities for N to B components.

question, we have performed a series of single QD experiments on CdSe/ZnS QDs spin coated onto a quartz substrate. We emphasize that due to nonergodicity issues we do not attempt to draw 1:1 conclusions when comparing single and ensemble QD observations. However, it has been explicitly shown that despite weak ergodicity breaking,[46,47] for example, blinking properties (of single QDs), can be closely mapped onto reversible photobleaching[58−60] and PL decay[61] of ensembles of QDs.

TABLE 1. QD PL Decay Times, τ_i, Normalized Amplitudes, A_i, and Intensities, I_i, for CdSe/ZnS and QDs in H_2P-CdSe/ZnS or CuP-CdSe/ZnS Nanoassemblies at T = 77 and 290 K[a]

				ensemble of QDs[a]					
		single QD[b] CdSe/ZnS		CdSe/ZnS		H_2P-CdSe/ZnS		CuP-CdSe/ZnS	
T/K	τ_i/ns, I_i/%, $E_{i,fwhm}$	high	low	high	low	high	low	high	low
77	τ_1			0.5		0.3		0.2	0.4
	A_1			0.2		0.51	0.56	0.9	0.7
	I_1			1		3	3	21	5
	τ_2			4	3.5	3.8	4	2.8	3.3
	A_2			0.28	0.2	0.27	0.21	0.07	0.2
	I_2			14	5	22	16	21	15
	τ_3			14.5	16	11.5	12.5	9.8	10.3
	A_3			0.52	0.8	0.31	0.35	0.03	0.1
	I_3			85	95	75	82	59	80
	$\langle\tau\rangle$[c]			14.5	17.5	9.5	10.5	9.0	8.5
290	τ_1	2	0.8	0.8	0.8	0.3	0.6	0.5	0.5
	A_1	0.13	0.44	0.37	0.33	0.72	0.65	0.63	0.64
	I_1			4	3	7	10	7	8
	τ_2	9	8	7.7	7	4	5	6	5
	A_2	0.31	0.27	0.36	0.36	0.15	0.2	0.19	0.17
	I_2			35	30	20	25	25	21
	τ_3	21	18	18	18	16.5	17.5	17	16.5
	A_3	0.56	0.29	0.27	0.31	0.13	0.15	0.18	0.17
	I_3			61	67	72	65	68	71
	$\langle\tau\rangle$[c]	13.9	14.4	14.5	14.5	12.5	12.0	12.5	11

[a] Parameter ranges (high, low) correspond to the variation of the QD PL detected at high and low PL energy at the corresponding fwhm of the PL band. Typical errors for τ_i are 0.2−0.5 ns. Typical errors for A_i are 5% (λ_{exc} = 410 nm in a methylcyclohexane/toluene (6:1) mixture). [b] Single QD data according to Figure 6B. Data have been taken for the peak values of the corresponding distributions. [c] Value of $\langle\tau\rangle$ has been calculated according to eq 2 (see Methods).

It is well-known that QDs show a strong PL intermittency (blinking) on time scales of milliseconds to seconds.[43,45,62,63] We analyzed blinking events by the change point analysis (CPA),[28,64] which allows one to detect optical properties for each individual PL intensity of a single QD during a blinking time trace.[65] As we have shown recently, with an adequate time resolution,[28,64] PL intensities vary continuously during a blinking time trace covering high, "dim", and low PL intensities. A typical example for a blinking time trace is shown in Figure S6 (Supporting Information).

We also followed spectral diffusion of the PL of a single QD (detected *via* energy jumps ΔE between two spectrally separated detection channels using a dichroic beam splitter) as a function of the intermittent PL intensity during a blinking time trace, as shown in Figure 4 (top). Two observations immediately emerge. First, the average PL energy at a given PL intensity (open circles) shifts (after an initial ≈10 meV "jump" to higher energies) by $\Delta E \approx 30$ meV to lower energy with decreasing PL intensity between the two given (blue) lines in Figure 4. The line on the right marks the maximum I_{max} of the PL intensity distribution given in the bottom part of Figure 4. The line on the left marks 0.1 I_{max}. This latter intensity corresponds to the limit at which we can, for sensitivity reasons, discriminate between different spectral components in an ensemble experiment. Second, for a given PL intensity, we obtain, as is shown in Figure 4 (middle), a Gaussian distribution σ of spectral energies (spectral diffusion) of $\sigma \approx 20-30$ meV at a selected PL intensity during a blinking time trace, which is considerably broader than the experimental error but narrower than the typical fwhm of ≈130 meV observed in ensemble experiments.[9] Remarkably, σ becomes larger with decreasing intensity in the intensity range between the two blue lines in Figure 4.

We additionally performed time-resolved PL decay experiments on single QDs at 290 K as a function of PL intensity using two spectrally separated ("blue" and "red") detection channels. This provides information on the spectral distribution of PL decay components. Details are given in Supporting Information (Figure S2). The fitting results are included in Table 1.

Experiments on single porphyrin-related nanoassemblies would be desirable. However, they cannot be performed because one would have to identify the statistically formed assemblies *via* simultaneous identification of porphyrin and QD luminescence,[35] which is due to the small radiative rates of porphyrins that are not feasible.

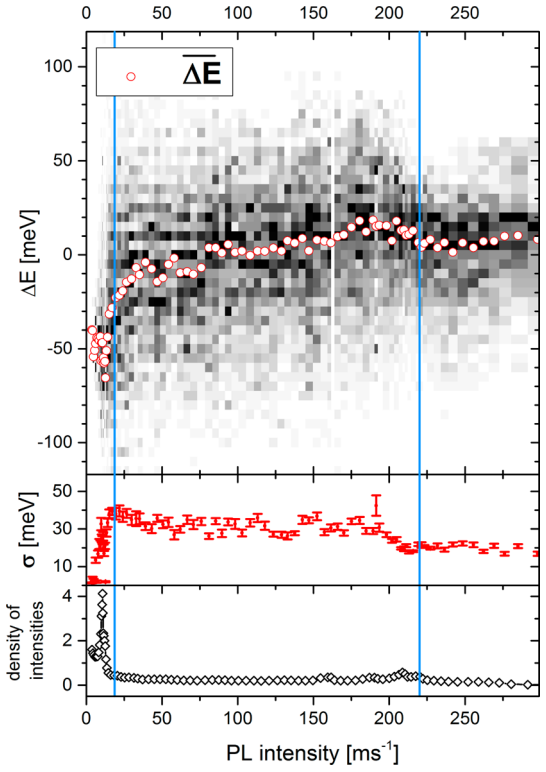

Figure 4. Top: Spectral jumps (diffusion) ΔE with respect to the dichroic beam splitter at 567 nm during a blinking time trace as a function of the PL intensity (determined by CPA) of a single CdSe/ZnS QD. Circles correspond to the algebraic average of fluctuating ΔE at the respective PL intensity. Blue lines indicate in the high intensity range the maximum of the intensity distribution (bottom) and at 1/10 of it. The latter corresponds to an intensity still detectable in continuous wave PL spectra. The spectral shift between these two marks is typically ≈35 meV. Middle: σ corresponds to the Gaussian width of the spectral diffusion at a given PL intensity and is typically 20−40 meV in the intensity range between the two blue lines. Bottom: Density of intensities as a function of PL (blinking) intensity as determined during a blinking time trace of the PL of a single QD.[28]

DISCUSSION

Previously, we have related non-FRET PL quenching to the extension of the excitonic wave function beyond the core/shell structure of the respective QDs[48] in combination with an appropriate ligand removal.[35−37,39] Now it is time to investigate related modifications on a microscopic level in order to identify the energies of electronic states that are generated or modified *via* the attachment (detachment) of appropriate dye molecules (or ligands). The central goal of the discussion is to identify the influence of only one surface-attached dye molecule on the energy landscape of QD surface states. Naturally, the influence will be small. However, it will be of interest whether experimental results can be at least qualitatively compared with recent calculations on the influence of the replacement of (single) ligands on PL energies of QDs.[18−26]

Before starting the detailed discussion, we summarize a few prerequisites:

(i) Throughout the discussion, we will make use of—if appropriate—information gained from both single QD and ensemble spectroscopy. Justification of this approach is discussed in Supporting Information.

(ii) While in ensemble experiments size distribution adds to the inhomogeneous spectral width, spectral diffusion clearly identified for single QDs will additionally broaden inhomogeneously the width of an ensemble of QDs. Table S1 (Supporting Information) summarizes estimations of contributions to the spectral width of ensembles.

(iii) The formation of nanoassemblies as such is not in the focus of our interest since we[30,33−39,48] and others[31,40−42] have shown ample evidence of self-assembling processes. However, a quantitative interpretation of the present results has to take into account that nanoassembly formation is a dynamic process including ligand (TOPO) exchange dynamics and dye attachment (at least in liquid solutions).[35,36,66−68] As is shown in the Supporting Information, the equilibrium constant of TOPO ligands is smaller than that of porphyrins. We have estimated that, related to steric constraints, at least three TOPO molecules have to be replaced to allow for the attachment of one *tetra*-pyridyl porphyrin molecule.[30,36] We have further found that at $x = 1$ only about 1/5 of the porphyrin molecules are attached to the QD surface in equilibrium.[30,35] This low attachment efficiency ensures that not all QDs form nanoassemblies at ambient temperature. This implies that following a Poisson distribution at most one porphyrin is attached to the QD surface. However, decreasing temperature will increase the concentration of nanoassemblies because of the increase of the complexation constant.[36,37] For these reasons, the spectral deconvolution of the PL of QDs in nanoassemblies has, in principle, to take into account the (temperature-dependent) superposition of PL energies of both CdSe/ZnS and QDs in nanoassemblies.

(iv) As became already evident by a quantitative inspection of PL parameters of QDs, there is a sudden change of the parameters close to $T_{crit} \approx 220$ K, which is related to a phase transition within the capping ligand moiety as has been identified for various ligands[55−57] as well as by us for CdSe/ZnS QDs capped by long-chain amines (Figure S5 Supporting Information).[50] In comparison with CdSe/ZnS, the PL intensity jump at T_{crit} is considerably enlarged upon attachment of a porphyrin molecule. We will not discuss the details of the phase transition in this paper but take it as a kind of marker at which the nature of PL states is switched with respect to both PL energies and dynamics (see also Table 1).

Deconvolution of the PL bands (Figure 1) into two Gaussian components (Figure 3) improves the fitting accuracy in comparison to fitting by one Gaussian component Figure 2). The limiting conditions for such a deconvolution are discussed in more detail in the

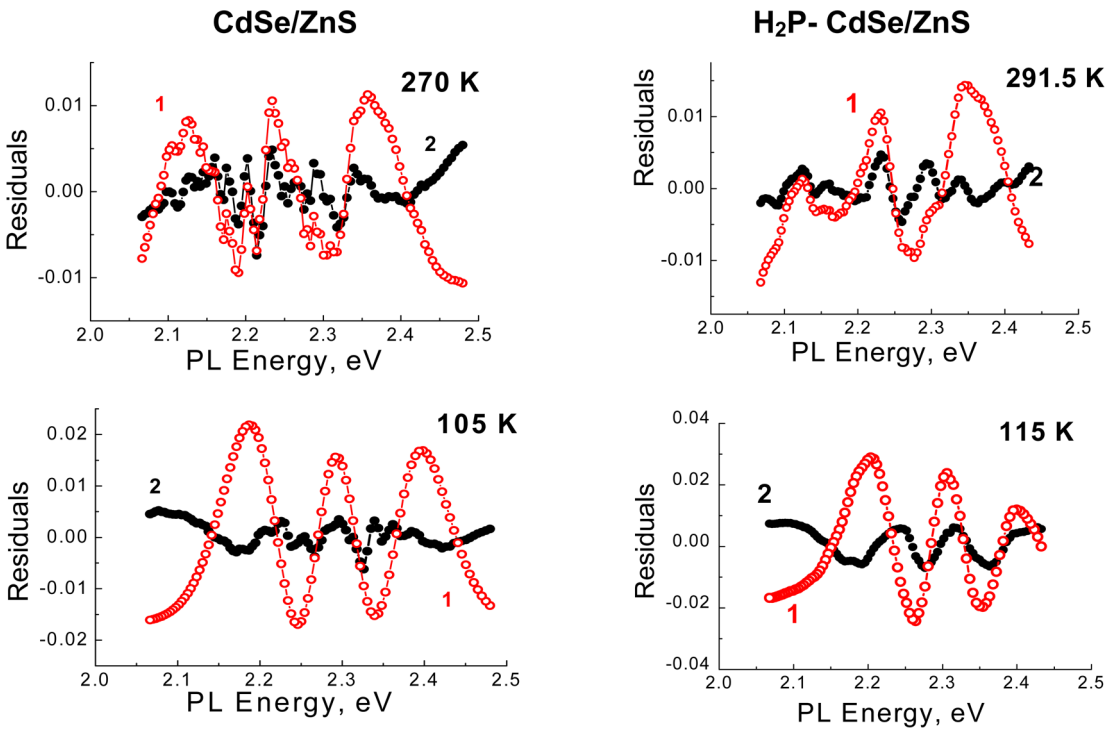

Figure 5. Exemplary fitting residuals for CdSe/ZnS and H_2P-CdSe/ZnS for QD PL bands fitted by one (red lines and residuals (1,○)) or two (black lines and residuals (2,●)) at high and low temperatures. PL band intensities have been normalized to 1 with respect to the maximum. Residuals are shown for normalized PL band intensity. The corresponding fitting parameters (reduced χ_R values and coefficients of determination R^2), fitting results for CuP-CdSe/ZnS, and data at additional temperatures are presented in the Supporting Information.

Supporting Information. Figure 5 shows a compilation of the fitting accuracy (residuals) for PL of CdSe/ZnS and QDs in H_2P-CdSe/ZnS nanoassemblies at two typical temperatures. A larger set of data is shown in the Supporting Information. We have calculated the confidence interval to be ±1.5 meV for the most conclusive parameters, the PL energies (for details see Supporting Information). Comparing the residuals for one Gaussian and two Gaussian fits in Figure 5 clearly shows that they are considerably improved especially in the low temperature range. Surprisingly, for QDs in CuP-CdSe/ZnS, the improvement for a two-component fit is less pronounced (see Table S2 in Supporting Information) despite the fact that in the latter case a very pronounced change is observed especially for the fwhm when comparing PL of CdSe/ZnS and QDs in CuP-CdSe/ZnS. We take this as a strong indication that, at least in this case, even more than two components should be considered (at low temperatures). Differences ΔE among fitted PL energies $(E_{max})_i$ are more pronounced in the low temperature range (Figure 3), which improves the fitting accuracy in combination with the observed overall line narrowing.

With these remarks in mind, we concentrate our discussion now on the fact if and how only one specific porphyrin molecule being attached to a QD surface tunes the electronic properties of a CdSe/ZnS QD. It is immediately evident from Figure 2 that, at least in the low temperature range, new PL energies and spectral broadening emerge that are several tens of millielectronvolts distinct from the original QD PL.

Correlation of PL Energies and PL Decay Dynamics in Ensembles of QDs. Additional information on assembly formation stems from time-resolved PL decay experiments. The spectrally selected PL decay clearly shows an energetic distribution of PL energies depending on the specific surface-attached molecule (see Table 1 and Scheme S1 of Supporting Information). In fact, recent careful investigations have shown that PL decay times are broadly distributed[28,35,38] and depend on detection wavelength,[38] PL intensity,[65,70−72] and temperature.[69] Therefore, assignment of at least three different PL decay times is an approximation in agreement with many previous results on CdSe/ZnS QDs.[28,30,35,36,38,69−72] Petrov *et al.* have explicitly shown that three main (broadly distributed) decay times can be explained by decay dynamics longer than about 0.5 ns and that this distribution is modified distinctively by dye attachment.[30,38]

In the following, we will in a first step correlate the results from spectral deconvolution (Figure 3) with those for the PL decay analysis (Table 1, Scheme S1, and Figure S1). To the best of our knowledge, a spectral deconvolution into two spectral components has not been achieved before across such a broad temperature range. Applying spectral deconvolution, one has to take into account that a considerable part of the respective line width of the PL band stems from size

distribution (see Table S1). We postulate that each individual QD (at a given size) has a (well-defined) set of PL state energies with associated (different) PL decay times. All our ensemble experiments have been performed at low excitation power, which minimizes the contribution of multiexcitons. Moreover, from single QD data (see Figure 4), we know that QDs are subject to spectral diffusion, which adds additionally to the inhomogeneous fwhm (see Table S1). The interplay of various contributions (constituting the inhomogeneous line width) implies that PL from a distinct electronic state (with a closely related decay time) will be distributed across the total inhomogeneous line width. Nevertheless, PL decay times are not equally distributed across the fwhm, as can be seen in Table 1, Figure S1, and Scheme S1. Basically, the contribution of short decay times increases with PL energy, especially at low temperatures.

At first glance, the identification of two spectral components is in contrast to the identification of three PL decay times. However, it has to be taken into account that the analysis of the PL decay provides the percentage contribution A_i of each decay (electronic state) component. Contrary, continuous time spectroscopy relies on intensities I_i (see Table 1 and Scheme S1) and is thus less sensitive to states with short-lived PL (at least for comparable radiative rates). Based on recent experiments, we assume throughout this paper that radiative decay rates differ by at most a factor of 2.[28] Inspection of Table 1 reveals that the integrated intensities I_i of the fastest decaying component ($\tau_1 < 1$ ns) are in most cases less than 10% of the total intensity and will therefore not contribute noticeably to $\langle\tau\rangle$ (see eq 2 and Figure S1) or to the QD PL spectra. There is only one exception, namely, for CuP-CdSe/ZnS nano assemblies at 77 K, which we will discuss separately later on. The relation of decay components with respect to the distribution of PL energies is shown qualitatively in Schemes S1 and S2.

Comparison of Ensemble and Single QD Data. Before we discuss the assembly-related modifications of PL energies in more detail, we state that the variation of PL energies and decay times is not merely due to a distribution of properties of different individual QDs. Our working hypothesis is that each QD within the ensemble explores subsequently in time the various states differing in PL energy and decay time. We did not observe build-up components of the PL decay longer than the intrinsic time resolution of about 0.2 ns.[28,30,38] Therefore, internal transfer processes such as energy transfer among individual energy levels of a single QD can be safely excluded. In close relation to blinking processes observed for single QDs,[28,43−45] PL subsequently originates on slow time scales from different electronic states, such as charged/uncharged QDs. As we outline in Supporting Information in more detail, we conclude that ensemble and single QD data can be qualitatively mapped on each other.

An analysis of the spectral shifts ΔE and spectral fluctuations σ collected in Figure 4 provides CdSe/ZnS information on the distribution of PL energies, with the viewpoint of single CdSe/ZnS or ensembles of QDs. Low PL intensities in the course of a blinking time trace correlate with short PL decay times and low PL energies. When a multiexponential PL decay is taken into account (Figure S2), up to three different emitting states contribute to a selected PL intensity.[28] We have identified recently that the long decay time τ_3 is related to the highest PL intensity I_{max}, while τ_2 relates to intensities about 10−20% lower than I_{max}.[28] This corresponds, for the QD shown in Figure 4, to an energy shift of $\approx$+10 meV and a related broadening of σ by about 10 meV (at the right blue line in Figure 4). The shortest time τ_1 is identified to occur predominantly at intensities of about 10% of I_{max} (blue line on the left).[28] This component is further shifted by +10 meV to higher energies (superimposed on the general red shift typical for low intensities) as is suggested by the peaked increase of σ at this low intensity, which we take as an indication of a third distinct electronic state at still higher PL energies as has been suggested recently including time-resolved experiments.[28]

Concluding, we find from single QD data three characteristic energies separated by typically 10 meV with three closely related PL decay times (Table 1) of about 1, 8, and 18 ns. PL decay times increase with decreasing PL energies. These findings are very close to those found for ensembles of QDs following deconvolution of PL spectra and decay times. It should be noted that—besides QDs in CuP-CdSe/ZnS—the short-lived component is not identified following spectral deconvolution.

Assignment of PL Energies in Nanoassemblies. Now we turn to our central goal, namely, to explain the origin of at least two different spectral PL components of CdSe/ZnS or the related nanoassemblies. According to our prerequisite (iii), we have to take into account that not all QDs are involved in nanoassembly formation. To approach this problem, we show in Figure 6A the temperature dependence of PL energies $(E_{max})_i$ of QDs in H_2P-CdSe/ZnS nanoassemblies (data points for N and B components) together with the energetically averaged values E_{max} for CdSe/ZnS (black solid line). From a comparison, we realize that the low energy component of QDs in H_2P-CdSe/ZnS nanoassemblies follows nearly exactly the temperature behavior of the averaged E_{max} of CdSe/ZnS. For this reason, we assign this latter component mainly to uncomplexed QDs. Following this assignment, the integrated PL intensity ratio is $I_{CdSe/ZnS}/I_{H_2P\text{-}CdSe/ZnS} \sim I_N/I_B \approx 3.5$ (see Figure 3D) at 295 K, which is reasonably close to the "formation" ratio of 4 as discussed in prerequisite (iii). The intensity ratio changes to $\approx$1.2 at 90 K.

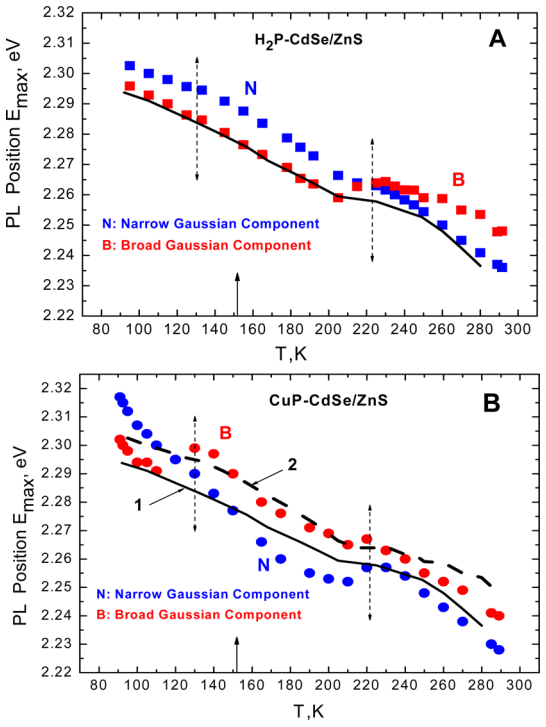

Figure 6. Comparison of temperature-dependent QD PL energy maxima $(E_{max})_i$ for various nanoassemblies. (A) PL energies for H_2P-CdSe/ZnS nanoassemblies (squares for N and B components taken from Figure 3) and for CdSe/ZnS QDs (solid line representing averaged data taken from Figure 3 for the two Gaussian components). (B) PL energies for CuP-CdSe/ZnS nanoassemblies (dots for N and B components taken from Figure 4), for CdSe/ZnS QDs (solid line 1 representing averaged data taken from Figure 3 for the two Gaussian components), and for the energetically high spectral component of QD PL in H_2P-CdSe/ZnS nanoassemblies (dashed line 2 taken from Figure 6A). Glass transition temperature for a methylcyclohexane/toluene (6:1) mixture is shown by an arrow (solid line). The temperature T_{crit} (≈220 K) of a phase transition of the capping TOPO layer is indicated by a dashed arrow. An discontinuity of some energies is found at $T \approx 130$ K (indicated by a second dashed arrow).

This corresponds to a situation in which ≈1/2 of the H_2P molecules are involved in assembly formation. We find that an attached H_2P induces at least one new emissive CdSe/ZnS state, which is at all temperatures higher in energy than the one of CdSe/ZnS. This assignment applies if the two PL bands belong either to CdSe/ZnS or to H_2P-CdSe/ZnS. At T_{crit}, some of the lowest states are shifted up in energy (see Scheme S2), which is manifested as an abrupt increase (reduced quenching) of the QD PL intensity (see Figure 2A,B).

To continue with CuP-CdSe/ZnS nanoassemblies, we compare in Figure 6B the temperature dependence of values $(E_{max})_i$ for N and B components (data points) with the (averaged) one for CdSe/ZnS (black solid line) and with the highest energy of QD PL in H_2P-CdSe/ZnS nanoassemblies (dashed line). It is evident that the overall spectral behavior is quite different for this type of nanoassembly as compared to H_2P-CdSe/ZnS. Remarkably, the temperature dependence is noticeably different compared to individual PL energies. At temperatures above T_{crit}, the energetically lowest components of QDs in H_2P-CdSe/ZnS and CuP-CdSe/ZnS nanoassemblies nearly coincide with the ones of CdSe/ZnS, while the high energy components B of QDs in the two nanoassemblies differ among each other.

Below T_{crit}, energies $(E_{max})_i$ vary considerably between the two nanoassemblies. There is definitely a different temperature behavior for QD PL in CuP-CdSe/ZnS nanoassemblies (blue dots in Figure 6B) as compared to QDs in H_2P-CdSe/ZnS (dashed line). Two separated temperature ranges emerge. Below $T \approx$ 130 K, we find that $(E_{max})_i$ for CdSe/ZnS-CuP is higher than $(E_{max})_i$ for CdSe/ZnS-H_2P. In the range $T >$ 130 K, the high energy components of CuP-CdSe/ZnS (red dots in Figure 6B) and H_2P-CdSe/ZnS (dashed line) are quite similar to each other. Contrary, the low energy component of CuP-CdSe/ZnS (blue dots in Figure 6B) follows neither the temperature dependence of CdSe/ZnS nor the one of QDs in H_2P-CdSe/ZnS nanoassemblies. In addition, the temperature dependence of one of the energy components of QD PL in CuP-CdSe/ZnS nanoassemblies has steeper temperature dependence compared to all the other components. It apparently "crosses" the energies of the second component of QD PL in CuP-CdSe/ZnS nanoassemblies at $T \approx$ 120−130 K. Such steep temperature dependence might be related to a strongly polar or charge characteristic of this state, thus being very sensitive to temperature-dependent electron−phonon coupling. When the (averaged) energetic component of uncomplexed QDs is taken into account again, at least two specifically CuP-related new states show up: one of the states (red dots) is similar to the state related to H_2P attachment ($\tau_2 \approx$ 3−4 ns); the other one is a short-lived state with $\tau_1 <$ 0.5 ns (blue dots). Scheme S2 (Supporting Information) shows qualitatively the temperature dependence of PL energies together with the assigned PL decay times. A compilation of all these findings with respect to PL energies demonstrates that all PL stems from states below the band-edge energy and has to be assigned to intrinsic or induced surface or trap states.

In Figure 7, we compare Stokes shifts of CdSe/ZnS and QDs in H_2P-CdSe/ZnS. Corresponding shifts for QDs in CuP-CdSe/ZnS have also been obtained (Figure S10 in Supporting Information) but are very complex because—as already discussed—the related two-Gaussian deconvolution is an obvious oversimplification. Stokes shifts have been obtained between the PL energies and the lowest energy of absorption. We did not find changes in absorption following assembly formation. As expected, all Stokes shifts show at T_{crit} a jump in energy. The Stokes shift of 22 meV is temperature-independent above T_{crit} for CdSe/ZnS, which indicates that both absorption and PL emission belong to states of the same nature. Below T_{crit}, shifts are temperature-dependent as one would expect in case of Boltzmann equilibration among fine structure

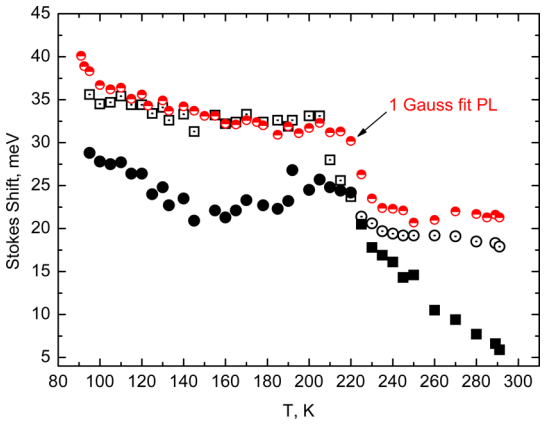

Figure 7. Temperature-dependent Stokes shifts of CdSe/ZnS (red/white dots) and QDs in H_2P-CdSe/ZnS. Shifts for CdSe/ZnS have been obtained between the PL deconvoluted by one Gaussian and the lowest absorption band. Data for the two individual components (see Figure 3) for CdSe/ZnS and QDs in CuP-CdSe/ZnS are shown in Supporting Information. Stokes shifts of QDs in H_2P-CdSe/ZnS are assigned either to CdSe/ZnS (open symbols) or to QDs in nanoassemblies (filled symbols). Squares correspond to broad bands B and dots to narrow bands N.

states.[73] The by 10−18 meV increased Stokes shift in this temperature range corresponds to a change in surface state energies.

With respect to the Stokes shifts of QDs in H_2P-CdSe/ZnS, we apply the same distinction between noncomplexed QDs and those in assemblies, as discussed with respect to Figure 6. Accordingly, we find two different shifts, as shown in Figure 7. While the shifts related to uncomplexed QDs are nearly identical to those of CdSe/ZnS, the ones assigned to nanoassemblies differ considerably. Stokes shifts in nanoassemblies depend above T_{crit} nearly linearly on temperature, indicating that the related states are less sensitive to electron−phonon coupling as compared to CdSe/ZnS. This may tentatively be explained by a stronger localization of the wave function, as expected for trap states. Below T_{crit}, the temperature dependence is complex, revealing a change in temperature dependence close to the glass transition temperature of the matrix at T_G = 151.6 K. We suggest that below T_G all molecular motion is frozen followed by a fixed two-fold coordination of H_2P on the QD surface, giving rise to a similar linear temperature dependence as that above T_{crit}. Above T_G, relaxation of the configuration of the nanoassembly might still be possible, giving rise to a variation of energetically different configurations (see also Scheme 2).

In principle, photoluminescence excitation spectra might provide more specific insights on assembly-related absorption energies. We have performed such experiments which, unfortunately, did not provide any of the expected information. Details of this failure are given in Supporting Information (Figure S12).

Comparison with Calculations. How can the observed modification of PL energies upon assembly formation be interpreted? Recent calculations have shown that energies of band-edge states of QDs depend on ligand attachment (saturation of dangling bonds),[17,20] solvent,[24] and dye attachment.[21] We have previously shown that QD−dye self-assembly will result in QD PL quenching (and modification of blinking), which is related neither to FRET nor to charge transfer.[30,35,36] From this point of view, it is not surprising, though experimentally shown for the first time, that only one dye molecule is capable of changing the surface-related distribution of near-band-edge or surface state energies. In some respect, this might be explained by the extension of the exciton wave function beyond the core/shell structure of the respective QD.[48,74] It is within this context only a matter of semantics to assign such states either to band-edge states, surface states, or shallow traps.

Using density functional theory (DFT) and time-dependent DFT quantum mechanical methods, it has recently been shown that ligands such as $OPMe_3$ (TOPO-like), NH_2Me (amine-like), and pyridine introduce new states to the QD band-edge states of both the conduction and valence bands.[20,22] The energies of these new states depend on the number and kind of ligands as well as on the position of the ligands with respect to the QD crystal structure.[20] Though calculations have been performed on rather small $Cd_{33}Se_{33}$ crystals, we suggest that the described behavior applies also at least qualitatively to larger QDs. According to calculations and depending on the relative coverage by ligands, the lowest absorption energies shift in the range of ±200 meV to either low (high coverage) or high energies (low coverage).[20] Most importantly, with respect to the present results, the removal of only one ligand out of an initially symmetric set of ligands will shift the lowest absorption noticeably to higher or lower energies, strongly depending on the type of coordination of the removed ligand.[20,22,24]

Only about 30% of the dangling (Zn) bonds of the investigated CdSe/ZnS QDs (d_{CdSe} = 3.0 nm, 2 ZnS monolayers) are "saturated" by TOPO ligands due to ligand-related steric constraints, leaving a considerable part of the surface unsaturated and thus increasing the contribution of surface states.[35,75−77] Scheme 2 shows qualitatively how the lowest band-edge states respond to depletion of the ligand shell either due to geometric constraints or ligand replacement following dye attachment. We have estimated that an attached porphyrin molecule replaces at least 3 TOPO molecules thus introducing a pronounced asymmetry in the (remaining) TOPO ligand shell.[35,36] Our experimental finding of new porphyrin-induced PL energies shifted by up to 30 meV to higher PL energies (as compared to CdSe/ZnS) is (as can be seen in Figure 6) both above and below T_{crit}, in agreement with these predictions. The influence of the chromophoric porphyrin electronic states is negligible since porphyrins attach,

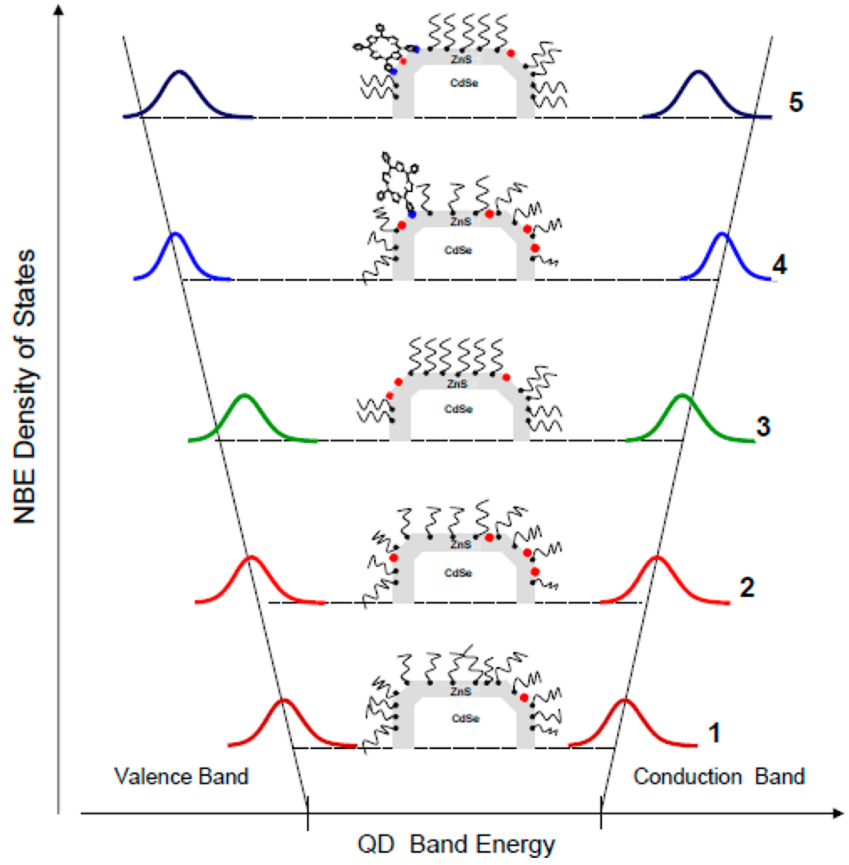

Scheme 2. Schematic presentation of the density of near-band-edge states as a function of ligand coverage (1−3), phase transition *via* ligand crystallization (3,5), and porphyrin attachment (4,5). Red dots indicate dangling bonds; blue dots indicate coordination of the porphyrin molecule *via* the *meso*-pyridyl ring to the QD surface. Increase of the band gap upon ligand depletion follows recent calculations by Kilina *et al.*[20,22] The phase transition is accompanied by creation of surface traps due to strain formation and increased ligand coverage. The transition from 3 to 4 is tentatively accompanied by a transition from a one-fold coordination of *tetra*-pyridyl-substituted porphyrin to a two-fold one. Qualitative presentation for the density of near-band-energy states as a function of CdSe/ZnS QD surface organization (based on considerations described in refs 20 and 22); (1) complete coverage of QD surface by capping ligand molecules; (2) partial coverage of QD surface by capping ligand molecules caused by steric constraints; (3) phase transition of capping layer (*e.g.*, crystallization and ordering) followed by the formation of additional surface defects; (4) competing attachment of a porphyrin molecule on QD surface before phase transition, leading to the removal of few capping ligand molecules due to steric interactions; (5) competing two-point attachment of a porphyrin molecule on QD surface after phase transition in the vicinity of surface defects.

as is shown in Scheme 1, in a nearly upright orientation with respect to the QD surface.[30]

Naturally, assemblies are much more complex than to be described in such a simple fashion. However, the general feature to generate new blue-shifted states when replacing TOPO ligands with pyridine-type ligands is in qualitative agreement with theoretical predictions.[20,22,24] The experimentally observed generation of new QD states is most pronounced for CuP-CdSe/ZnS nanoassemblies, probably because of an additional steric influence due to ligation of the central Cu ion of porphyrin by TOPO (see Supporting Information) accompanied by removal of additional ligands, as is shown schematically in Scheme 1 (II B). Removal or replacement of ligands will give rise to an enhancement of radiationless transitions. The complexation with a dye molecule will locally disturb the symmetry and/or trapped charge distribution at the surface of a QD.[48] In line with this, Al Salman *et al.* have recently made the proposal that lowering the symmetry of the QD (or its surface) will intermix QD fine structure states, giving rise to variations in the PL decay channels.[69]

The present experiments have been performed on CdSe/ZnS QDs, whereas most of the calculations are reported for (small) CdSe QDs without a shell.[19,24−26] However, more recent calculations include both CdSe core and ZnS shell states.[78] As expected, a new set of density of states is created in such systems without a clear distinction between CdSe and ZnS states. Remarkably, the ZnS shell creates predominantly additional states near the band-edge of the CdSe valence band, which implies that holes are localized in the ZnS shell but electrons remain in the CdSe core. This enhances electron−hole separation and results in a reduction of nonradiative relaxation processes. Presence of defects in the shell (ligand or atom removal) will predominantly transfer the hole back into the CdSe core,

thereby relaxing the electron−hole decoupling, which finally results in enhanced (electron−phonon) relaxation processes.[78] We propose that the experimentally observed increase of nonradiative PL decay (PL quenching) upon porphyrin attachment is related to an increase of surface defects at the valence band-edge trapping holes close to the ZnS−pyridyl coordination.

Naturally, the influence of assembly formation should depend on QD size and ZnS shell thickness. We have recently shown that the magnitude of porphyrin-induced PL quenching can, in fact, be quantitatively described by an extension of the excitonic wave function beyond the CdSe core, thus critically depending on QD size and shell thickness.[48] An experimental investigation on the related impact on electronic energies in the case of nanoassemblies is left for future experiments.

Relation of Ligand Phase Transition and Dye-Induced PL Quenching. Finally, we discuss the behavior of the PL properties at T_{crit}, which is a kind of phase transition of the ligand shell.[50,55−57] Since it is also present for CdSe/ZnS QDs, it is primarily not caused by the porphyrins, though the effects on QD PL intensities and decay times are dramatically influenced in the case of assembly formation.

Meijerink *et al.* have shown that at a critical temperature an ordering ("crystallization") of the ligand layer (especially of the aliphatic side chains) takes place, causing strain to the crystal surface.[55−57] Such strain will result in an increase of surface-related trap states, accompanied by a modification of PL dynamics and thus PL intensity. Scheme 2 demonstrates qualitatively the influence of ligand "crystallization", resulting in surface trap state PL within the band gap for both CdSe/ZnS and QDs in nanoassemblies. Such a phase transition is tentatively similar to the calculated formation of intraband states following the removal of only one (or a few) ligand molecule.[18,20,22] As long as the ligand shell is quite flexible above T_{crit}, assembly formation results in quenched PL accompanied by a formation of blue-shifted trap states.

At the phase transition, the energetic order of surface and surface trap states is exchanged and the dynamics are modified as indicated by decreased PL decay times below T_{crit} as compared to the ones above T_{crit}, opposite of what is expected for temperature-activated relaxation processes such as electron−phonon coupling.

With respect to the dramatically increased PL quenching at T_{crit} and below, Scheme 2 provides a qualitative explanation. We suggest that the formation of a partially crystalline structure of the ligand shell causes the porphyrin to more effectively contact the QD surface, for example, from a one-fold to a two-fold pyridyl coordination. As a consequence, nonradiative decay channels are dramatically increased by trapping holes at the surface sites of pyridyl surface attachment. It is well-known that the analogous pyridine or pyrazine molecules are effective hole acceptors.[79] Similar enhancement of PL quenching at the phase transition is observed also for (pyridyl)$_2$−perylene diimide dye molecules on CdSe/ZnS QDs ligated by long-chain amines.[50]

Finally, we interpret qualitatively the apparent crossing of PL energies of QDs in CuP-CdSe/ZnS nanoassemblies in the vicinity of $T \approx 130$ K. Noncontinuous changes in PL lifetimes (and thus correlated PL intensities) upon temperature variation have been investigated by Scholes *et al.*[80,81] Depending on QD size, they found up to two PL decay time minima, which they explained by a temperature-dependent competition of trap state distributions.[81] Though not investigated previously, similar variations with temperature should also show up in the distribution of PL energies. We speculate that our experimental observations at $T \approx 130$ K might be closely related to those reported findings.[82,83]

CONCLUSIONS

The combination of ensemble and newly designed single QD experiments allows for a detailed, and up to now not yet reported, complex analysis of the PL of QDs in CdSe/ZnS−dye nanoassemblies embedded in a glass matrix. In both cases, namely, ensemble- and time-averaged single QD detection, electronic states of different nature with varying PL energies and decay dynamics are subsequently explored on slow time scales typical for blinking phenomena, which are buried but nevertheless are present in ensemble experiments. Upon temperature variation, the ordering of at least two energetically deconvoluted PL states is abruptly changed at the phase transition.

The temperature dependence of the PL observables reveals both the influence of electron−phonon coupling between 77 and 290 K and a phase transition of the capping TOPO shell at $T_{crit} \approx 220$ K. According to time-resolved experiments, we find at least three basically different types of emissive states (see Table 1). Though we identified *via* spectral deconvolution only two PL energies, this is easily understood since the short PL decay component will, in most cases, not contribute significantly to the time-averaged PL spectrum.

Modifications of PL properties of nanoassemblies are assigned to dye-induced ligand removal accompanied by spectral blue shifts and formation of surface trap states in the band gap. Comparison of averaged and deconvoluted spectral PL properties of CdSe/ZnS and QDs in nanoassemblies proves that one attached porphyrin molecule not only causes PL quenching but also changes the energy landscape of the QD PL noticeably. Temperature controls the energetic ordering of electronic states. Especially below the phase

transition of TOPO ligands, PL energies depend critically on the type of the surface-attached porphyrin molecule. Also, CdSe/ZnS−diimide assemblies with amine ligands show qualitatively similar phenomena.[50]

This specific selectivity to the surface-attached dye molecule provides new and not yet reported experimental insights into QD surface properties. In this respect, a qualitative comparison with calculations on the basis of a time-dependent DFT approach, which takes the number, position, and chemical nature of ligands and their specific removal into account, explains qualitatively the observed modifications of PL energies and dynamics. The basic conclusion is that a dye molecule removes ligands from (specific) surface sites, thus acting as a new "ligand" and creating a modified set of new surface states.[17−24] This explains specifically why (non-FRET) PL quenching upon QD−dye nanoassembly formation is often not exclusively related to energy (FRET) or charge transfer.[30,31,35−39,48] In a certain way, we use dye molecules as single molecular surface probes.

In the future, increasing knowledge of specific interactions at the QD surface will add to the control of the complex interplay of the QD core and surface properties and will allow for a guided tailoring of optical features of semiconductors with respect to applications in photovoltaics and especially nanosensors.

METHODS

CdSe/ZnS Quantum Dots. Colloidal CdSe/ZnS core−shell semiconductor QDs (d_{CdSe} = 3.0 nm; 2 ZnS monolayers; $\lambda_{PL} \approx$ 555 nm) capped with *n*-trioctylphosphine oxide were obtained from Evident Technologies, Inc. (Troy, NY, USA). The absorbance of the QD starting solutions was adjusted to be lower than 0.1 OD at excitation and emission wavelengths in order to avoid nonlinear absorption and reabsorption effects in ensemble experiments. The concentrations varied in the range of (3−5) × 10^{-6} M. Stability and purity of the QD solutions were checked by measuring the quantum yield stability at least more than 3 h after preparation. TOPO-capped CdSe/ZnS QDs ($\lambda_{PL} \approx$ 567 nm) used in single QD experiments were slightly larger compared to those in ensemble experiments.

***meso*-Pyridyl-Substituted Porphyrins.** Functionalized pyridyl-substituted porphyrin molecules, such as 5,10,15,20-*meso*-*meta*-pyridyl porphyrins [H_2P(m-Pyr)$_4$ (or briefly H_2P) and its Cu complex (CuP), as well as *tetra*-phenylporphyrin molecules of the same structure but having simple *meso*-phenyl rings], were synthesized and purified according to known methods.[82,83] The chemical structures of the corresponding porphyrins are shown in Scheme 1 together with a schematic presentation of the mutual arrangement of a porphyrin macrocycle with respect to the QD surface. The porphyrin stock solution was prepared in toluene under ultrasonic treatment at 40 °C at concentrations in the range of (3−30) × 10^{-5} M.

Sample Preparation. QD−porphyrin nanoassemblies are formed at room temperature *via* one-step titration of a solution of QDs by porphyrin molecules at a molar ratio of [C_{Porph}]/[C_{QD}] = x = 1. It has been proven earlier by us that a controllable self-assembly of QDs with 5,10,15,20-*meso*-*meta*-pyridyl porphyrins with H_2P and CuP[30,36−38,48] or with other organic molecules with corresponding anchoring groups[33,35,39] is realized *via* Zn···*N*-pyridyl coordination of Zn atoms of the ZnS shell with nitrogen atoms of pyridyl substituents.

Temperature-dependent measurements (77−300 K) for QDs and QD−porphyrin nanoassemblies were carried out in a mixture of methylcyclohexane/toluene (6:1 composition; spectroscopic grade; Fluka SeccoSolv dried over a molecular sieve), forming an optical transparent rigid glass matrix at low temperatures. The respective glass transition temperatures are as follows: 146.7 K for methylcyclohexane and 180 K for toluene[84] and 151.6 K for methylcyclohexane/toluene (6:1) mixtures.[85,86]

Single QD samples are prepared by spin coating a toluene solution containing CdSe/ZnS QDs onto a quartz substrate.[28,35,62] Porphyrin−QD nanoassemblies cannot be investigated on a single assembly level because the porphyrin luminescence is too weak to be detected which would, however, be necessary to identify single assembly formation[35] (see Figure S7 in Supporting Information).

Spectral and Time-Resolved Measurements. Absorption spectra were recorded with a Shimadzu 3001 UV/vis or a Cary-500 M Varian spectrometer. Emission spectra were measured with a Shimadzu RF-5001PC spectrofluorophotometer including a home-built highly sensitive temperature variable laboratory setup described earlier.[34]

Time-resolved PL measurements on ensembles were performed in a time-correlated single photon counting mode under right-angle geometry using a laboratory spectrofluorometer equipped with computer module TCC900 (Edinburg Instruments) and light-emitting diodes PLS-8-2-130 (λ_{max} = 457 nm, fwhm ∼ 713 ps) or PLS-8-2-135 (λ_{max} = 409 nm, fwhm ∼ 990 ps; PicoQuant GmbH). QD PL multiexponential decay curves $A(t)$ were fitted by three components A_i according to

$$A(t) = \Sigma A_i \exp(-t/\tau_i) \quad (1)$$

Mean decay times $\langle\tau\rangle$ were calculated according to

$$\langle\tau\rangle = (\Sigma A_i \tau_i^2)/(\Sigma A_i \tau_i) \quad (2)$$

Unfortunately, we were not able to perform time-resolved experiments at all temperatures because samples were photochemically degraded compared to spectroscopy upon increased excitation power density over such a long measuring period. Here we restricted our experiments to 77 and 290 K.

Time and spectrally resolved single QD experiments have been carried out with a home-built setup.[28,64] Blinking of single QDs is analyzed following change point analysis, which allows for an intensity-resolved PL decay in the sub-nanosecond range.[64,65] Photons are counted in two channels spectrally separated by a dichroic beam splitter set at 567 nm, allowing for identification of spectral diffusion among the channels. Time resolution is 0.2 ns. Details of the setup are described elsewhere.[28,87]

Conflict of Interest: The authors declare no competing financial interest.

Acknowledgment. Financial support from DFG Priority Unit FOR 877 ("From Local constraints to macroscopic transport") as well as from Belarussian State Program for Scientific Research "Convergence 3.2.08—Photophysics of Bioconjugates, Semiconductor and Metallic Nanostructures and Supramolecular Complexes and Their Biomedical Applications" for E.I.Z. is gratefully acknowledged.

Supporting Information Available: Analysis of time-dependent PL decay and various contributions to the line width fwhm for ensembles and single QDs. Details of formation of CuP-CdSe/ZnS nanoassemblies and temperature dependence of the PL of spin-coated CdSe/ZnS QDs and CuP-CdSe/ZnS nanoassemblies on a quartz substrate. "Phase transition" of ligands for CdSe/ZnS QD capped by long-chain amines. Change point analysis of QD blinking and PL blinking of single CdSe/ZnS and QDs in H_2P-CdSe/ZnS nanoassemblies on a quartz substrate at 290 K. Gaussian deconvolution of QD PL spectra and relation of PL decay to spectral deconvolution. Fitting of QD PL bands by Gaussian components (procedure, fitting accuracy, confidence

interval). Comments on Poisson distribution, ligand exchange, and complexation constants for nanoassemblies based on CdSe-ZnS QDs and porphyrins. This material is available free of charge *via* the Internet at http://pubs.acs.org.

REFERENCES AND NOTES

1. McBride, J. R.; Pennycook, T. J.; Pennycook, S. J.; Rosenthal, S. J. The Possibility and Implications of Dynamic Nanoparticle Surfaces. *ACS Nano* **2013**, *7*, 8358–8365.
2. Kuno, M.; Lee, J. K.; Dabbousi, B. O.; Mikulec, F. V.; Bawendi, M. G. The Band Edge Luminescence of Surface Modified CdSe Nanocrystallites: Probing the Luminescing State. *J. Chem. Phys.* **1997**, *106*, 9869–9882.
3. Garrett, M. D.; Bowers, M. J.; McBride, J. R.; Orndorff, R. L.; Pennycook, S. J.; Rosenthal, S. J. Band Edge Dynamics in CdSe Nanocrystals Observed by Ultrafast Fluorescence Upconversion. *J. Phys. Chem. C* **2008**, *112*, 436–442.
4. Kambhampati, P. Unraveling the Structure and Dynamics of Excitons in Semiconductor Quantum Dots. *Acc. Chem. Res.* **2011**, *44*, 1–13.
5. Empedocles, S. A.; Bawendi, M. G. Influence of Spectral Diffusion on the Line Shapes of Single CdSe Nanocrystallite Quantum Dots. *J. Phys. Chem. B* **1999**, *103*, 1826–1830.
6. Müller, J.; Lupton, J. M.; Rogach, A. L.; Feldmann, J.; Talapin, D. V.; Weller, H. Monitoring Surface Charge Migration in the Spectral Dynamics of Single CdSe/CdS Nanodot/Nanorod Heterostructures. *Phys. Rev. B* **2005**, *72*, 205339.
7. Gomez, D. E.; van Embden, J.; Mulvaney, P. Spectral Diffusion of Single Semiconductor Nanocrystals: The Influence of the Dielectric Environment. *Appl. Phys. Lett.* **2006**, *88*, 154106.
8. Fernee, M. J.; Plakhotnik, T.; Louyer, Y.; Littleton, B. N.; Potzner, C.; Tamarat, P.; Mulvaney, P.; Lounis, B. Spontaneous Spectral Diffusion in CdSe Quantum Dots. *J. Phys. Chem. Lett.* **2012**, *3*, 1716–1720.
9. Cui, J.; Beyler, A. P.; Bischof, T. S.; Wilson, M. W. B.; Bawendi, M. G. Deconstructing the Photon Stream from Single Nanocrystals: From Binning to Correlation. *Chem. Soc. Rev.* **2014**, *43*, 1287–1310.
10. Brown, P. R.; Kim, D.; Lunt, R. R.; Zhao, N.; Bawendi, M. G.; Grossman, J. C.; Bulovi, V. Energy Level Modification in Lead Sulfide Quantum Dot Thin Films through Ligand Exchange. *ACS Nano* **2014**, *8*, 5863–5872.
11. Yu, W. W.; Wang, Y. A.; Peng, X. Formation and Stability of Size-, Shape-, and Structure-Controlled CdTe Nanocrystals: Ligand Effects on Monomers and Nanocrystals. *Chem. Mater.* **2003**, *15*, 4300–4308.
12. Munro, A. M.; Ginger, D. S. Photoluminescence Quenching of Single Nanocrystals by Ligand Adsorption. *Nano Lett.* **2008**, *8*, 2585–2590.
13. Ji, X.; Copenhaver, D.; Sichmeller, C.; Peng, X. Ligand Bonding and Dynamics on Colloidal Nanocrystal at Room Temperature: The Case of Alkylamines on CdSe Nanocrystals. *J. Am. Chem. Soc.* **2008**, *130*, 5726–5735.
14. Smith, A. M.; Nie, S. Semiconductor Nanocrystals: Structure, Properties, and Band Gap Engineering. *Acc. Chem. Res.* **2010**, *43*, 190–200.
15. Puzder, A.; Williamson, A. J.; Zaitseva, N.; Galli, G.; Manna, L.; Alivisatos, A. P. The Effect of Organic Ligand Binding on the Growth of CdSe Nanoparticles Probed by *Ab Initio* Calculations. *Nano Lett.* **2004**, *4*, 2361–2365.
16. Rempel, J. Y.; Trout, B. L.; Bawendi, M. G.; Jensen, K. F. Density Functional Theory of Ligand Binding on CdSe (0001), (000$\bar{1}$), and (11$\bar{2}$0) Single Crystal Relaxed and Reconstructed Surfaces: Implications for Nanocrystalline Groth. *J. Phys. Chem. B* **2006**, *110*, 18007–18016.
17. Frenzel, J.; Joswig, J. O.; Seifert, G. Optical Excitations in Cadmium Sulfide Nanoparticles. *J. Phys. Chem. C* **2007**, *111*, 10761–10770.
18. Inerbaev, T. M.; Masunov, A. E.; Khondaker, S. I.; Dobrinescu, A.; Plamadă, A.-V.; Kawazoe, Y. Quantum Chemistry of Quantum Dots: Effects of Ligands and Oxidation. *J. Chem. Phys.* **2009**, *131*, 044106.
19. Gomez-Campos, F. M.; Califano, M. Hole Surface Trapping in CdSe Nanocrystals: Dynamics, Rate Fluctuations, and Implications for Blinking. *Nano Lett.* **2012**, *12*, 4508–4517.
20. Kilina, S. V.; Ivanov, S.; Tretiak, S. Effect of Surface Ligands on Optical and Electronic Spectra of Semiconductor Nanoclusters. *J. Am. Chem. Soc.* **2009**, *131*, 7717–7726.
21. Kilin, D. S.; Tsemekham, K.; Zenkevich, E. I.; Prezho, O. V.; von Borczyskowski, C. *Ab Initio* Study of Transfer Dynamics from a Core–Shell Semiconductor Quantum Dot to a Porphyrin Sensitizer. *J. Photochem. Photobiol., A* **2007**, *190*, 342–351.
22. Kilina, S.; Velizhanin, K. A.; Ivanov, S.; Prezhdo, O. V.; Tretiak, S. Surface Ligands Increase Photoexcitation Rates in CdSe Quantum Dots. *ACS Nano* **2012**, *6*, 6515–6524.
23. Califano, M.; Gómez-Campos, F. M. Universal Trapping Mechanism in Semiconductor Nanocrystals. *Nano Lett.* **2013**, *13*, 2047–2052.
24. Fischer, S. A.; Crotty, A. M. M.; Kilina, S. V.; Ivanov, S. A.; Tretiak, S. Passivating Ligand and Solvent Contributions to the Electronic Properties of Semiconductor Nanocrystals. *Nanoscale* **2012**, *4*, 904–914.
25. Voznyy, O.; Sargent, E. H. Atomistic Model of Fluorescence Intermittency of Colloidal Quantum Dots. *Phys. Rev. Lett.* **2014**, *112*, 157401.
26. Voznyy, O. Mobile Surface Traps in CdSe Nanocrystals with Carboxylic Acid Ligands. *J. Phys. Chem. C* **2011**, *115*, 15927–15932.
27. Frantsuzov, P. A.; Volkán-Kacscó, S.; Jankó, B. Universality of the Fluorescence Intermittency in Nanoscale Systems: Experiment and Theory. *Nano Lett.* **2013**, *13*, 402–408.
28. Schmidt, R.; Krasselt, C.; Göhler, C.; von Borczyskowski, C. The Fluorescence Intermittency for Quantum Dot Is Not Power-Law Distributed: A Luminescence Intensity Resolved Approach. *ACS Nano* **2014**, *8*, 3506–3521.
29. Clapp, A. R.; Medintz, I. L. J.; Mauro, M.; Fisher, B. R.; Bawendi, M. G.; Mattoussi, H. Fluorescence Resonance Energy Transfer between Quantum Dot Donors and Dye-Labeled Protein Acceptors. *J. Am. Chem. Soc.* **2004**, *126*, 301–310.
30. Zenkevich, E.; Shulga, A.; Cichos, F.; Petrov, E. P.; Blaudeck, T.; von Borczyskowski, C. Nanoassemblies Designed from Quantum Dots and Molecular Arrays. *J. Phys. Chem. B* **2005**, *109*, 8679–8692.
31. Dayal, S.; Lou, Y.; Samis, A. C. S.; Berlin, J. C.; Kenney, M. E.; Burda, C. Observation of Non-Förster-Type Energy-Transfer Behavior in Quantum Dot–Phthalocyanine Conjugates. *J. Am. Chem. Soc.* **2006**, *128*, 13974–13975.
32. Dworak, L.; Matylitzky, V. V.; Ren, T.; Basche, T.; Wachtveitl, J. Acceptor Concentration Dependence of Förster Resonance Energy Transfer Dynamics in Dye–Quantum Dot Complexes. *J. Phys. Chem. C* **2014**, *118*, 4396–4402.
33. Gerlach, F.; Täuber, D.; von Borczyskowski, C. Correlated Blinking *via* Time Dependent Energy Transfer in Single CdSe Quantum Dot–Dye Nanoassemblies. *Chem. Phys. Lett.* **2013**, *572*, 90–95.
34. Zenkevich, E. I.; Sagun, E. I.; Knyukshto, V. N.; Stasheuski, A. S.; Galievsky, V. A.; Stupak, A. P.; Blaudeck, T.; von Borczyskowski, C. Quantitative Analysis of Singlet Oxygen ($^1O_2$) Generation *via* Energy Transfer in Bioconjugates Based on Semiconductor Quantum Dots and Porphyrin Ligands. *J. Phys. Chem. C* **2011**, *115*, 21535–21545.
35. Kowerko, D.; Schuster, J.; Amecke, N.; Abdel-Mottaleb, M.; Dobrawa, R.; Würthner, F.; von Borczyskowski, C. FRET and Ligand Related Non-FRET Processes in Single Quantum Dot–Perylene Bisimide Assemblies. *Phys. Chem. Chem. Phys.* **2010**, *12*, 4112–4123.
36. Blaudeck, T.; Zenkevich, E. I.; Abdel-Mottaleb, M.; Szwaykowska, K.; Kowerko, D.; Cichos, F.; von Borczyskowski, C. Formation Principles and Ligand Dynamics of Nanoassemblies of CdSe Quantum Dots and Functionalised Dye Molecules. *ChemPhysChem.* **2012**, *13*, 959–972.
37. Zenkevich, E. I.; Blaudeck, T.; Abdel-Mottaleb, M.; Cichos, F.; Shulga, A. M.; von Borczyskowski, C. Photophysical Properties of Self-Aggregated Porphyrin–Semiconductor Nanoassemblies. *Int. J. Photoenergy* **2006**, *2006*, 90242.

38. Petrov, E. P.; Cichos, F.; von Borczyskowski, C. Intrinsic Photophysics of Semiconductor Nanocrystals in Dielectric Media: Formation of Surface States. *J. Luminesc.* **2006**, *119–120*, 412–417.
39. Kowerko, D.; Krause, S.; Amecke, N.; Abdel-Mottaleb, M.; Schuster, J.; von Borczyskowski, C. Identification of Different Donor–Acceptor Structures *via* FRET in Quantum-Dot–Perylene Bisimide Assemblies. *Int. J. Mol. Sci.* **2009**, *10*, 5239–5256.
40. Issac, A.; Jin, S.; Lian, T. Intermittent Electron Transfer Activity From Single CdSe. *J. Am. Chem. Soc.* **2008**, *130*, 11280–11281.
41. Funston, A. M.; Jasieniak, J. J.; Mulvaney, P. Complete Quenching of CdSe Nanocrystals Photoluminescence by Single Dye Molecules. *Adv. Mater.* **2008**, *20*, 4272–4280.
42. Roy, R.; Hohng, S.; Ha, T. A Practical Guide to Single-Molecule FRET. *Nat. Methods* **2008**, *5*, 507–516.
43. Cichos, F.; von Borczyskowski, C.; Orrit, M. Power-Law Intermittency of Single Emitters. *Curr. Opin. Colloid Interface Sci.* **2007**, *12*, 272–284.
44. Riley, E. A.; Hess, C. M.; Reid, P. J. Photoluminescence Intermittency from Single Quantum Dots to Organic Molecules: Emerging Themes. *Int. J. Mol. Sci.* **2012**, *13*, 12487–12518.
45. Cordones, A. A.; Leone, S. R. Mechanisms for Charge Trapping in Single Semiconductor Nanocrystals Probed by Fluorescence Blinking. *Chem. Soc. Rev.* **2013**, *42*, 3209–3221.
46. Kuno, M.; Fromm, D. P.; Johnson, S. T.; Gallagher, A.; Nesbitt, D. J. Modeling Distributed Kinetics in Isolated Semiconductor Quantum Dots. *Phys. Rev. B* **2003**, *67*, 1253041.
47. Margolin, G.; Barkai, G. E. Nonergodicity of Blinking Nanocrystals and Other Lévy-Walk Processes. *Phys. Rev. Lett.* **2005**, *94*, 080601–080614.
48. Blaudeck, T.; Zenkevich, E. I.; Cichos, F.; von Borczyskowski, C. Probing Wave Functions at Semiconductor Quantum-Dot Surfaces by Non-FRET Photoluminescence Quenching. *J. Phys. Chem. C* **2008**, *112*, 20251–20257.
49. Sagar, D. M.; Cooney, R. R.; Sewall, S. L.; Dias, E. A.; Barsan, M. M.; Butler, I. S.; Kambhampati, P. Size Dependent, State Resolved Studies of Exciton–Phonon Couplings in Strongly Confined Semiconductor Quantum Dots. *Phys. Rev. B* **2008**, *77*, 2353211.
50. Zenkevich, E. I.; Stupak, A.; Kowerko, D.; von Borczyskowski, C. Influence of Single Dye Molecules on Temperature and Time Dependent Optical Properties of CdSe/ZnS Quantum Dots: Ensemble and Single Nanoassembly Detection. *Chem. Phys.* **2012**, *406*, 21–29.
51. Joshi, A.; Davis, E.; Narsingi, K.; Manasreg, O.; Weaver, B. D. Optical Properties of Colloidal CdSe/ZnS Core/Shell Nanocrystals Embedded in a UV Curavle Resin. *Mater. Res. Soc. Symp. Proc.* **2007**, *959*, M06-04.
52. Valerini, D.; Creti, A.; Lomascolo, M.; Manna, L.; Cingolani, R.; Anni, M. Temperature Dependence of the Photoluminescence Properties of Colloidal CdSe/ZnS Core/Shell Quantum Dots Embedded in a Polystyrene Matrix. *Phys. Rev. B* **2005**, *71*, 235409.
53. Ehlert, O.; Tiwari, A.; Nann, T. Quantum Confinement of the Thermodynamic Functions for the Formation of Electrons and Holes in CdSe Nanocrystals. *J. Appl. Phys.* **2006**, *100*, 074314.
54. Morello, G.; de Giorgi, M.; Kudera, S.; Manna, L.; Cingolani, R.; Anni, M. Temperature and Size Dependence of Nonradiative Relaxation and Exciton–Phonon Coupling in Colloidal CdTe Quantum Dots. *J. Phys. Chem. C* **2007**, *111*, 5846–5849.
55. Wuister, S. F.; de Mello Donega, C.; Bode, M.; Meijerink, A. Luminescence Temperature Antiquenching of Water-Soluble CdTe Quantum Dots: Role of Solvents. *J. Am. Chem. Soc.* **2004**, *126*, 10397–19402.
56. Wuister, S. F.; van Houselt, A.; de Mello Donega, C.; Vanmaekelbergh, D.; Meijerink, A. Temperature Antiquenching of the Luminescence from Capped CdSe Quantum Dots. *Angew. Chem., Int. Ed.* **2004**, *43*, 3029–3033.
57. de Mello Donega, C.; Bode, M.; Meijerink, A. Size- and Temperature-Dependence of Exciton Lifetimes in CdSe Quantum Dots. *Phys. Rev. B* **2006**, *74*, 085321–085329.
58. Chung, I.; Bawendi, M. G. Relationship between Single Quantum-Dot Intermittency and Fluorescence Intensity Decays from Collections of Dots. *Phys. Rev. B* **2004**, *70*, 165304.
59. Cichos, F.; Martin, J. C.; von Borczyskowski, C. Emission Intermittency in Silicon Nanocrystals. *Phys. Rev. B* **2004**, *70*, 1153141.
60. Schuster, J.; Brabandt, J.; von Borczyskowski, C. Discrimination of Photoblinking and Photobleaching on the Single Molecule Level. *J. Luminesc.* **2007**, *127*, 224–229.
61. Tachiya, M.; Seki, K. Unified Explanation of the Fluorescence Decay and Blinking Characteristics of Semiconductor Nanocrystals. *Appl. Phys. Lett.* **2009**, *94*, 0811041–0811043.
62. Krasselt, C.; Schuster, J.; von Borczyskowski, C. Photoinduced Hole Trapping in Single Semiconductor Quantum Dots at Specific Sites at Silicon Oxide Interfaces. *Phys. Chem. Chem. Phys.* **2011**, *13*, 17084–17092.
63. Issac, A.; Krasselt, C.; Cichos, F.; von Borczyskowski, C. Influence of the Dielectric Environment on the Photoluminescence Intermittency of CdSe Quantum Dots. *ChemPhysChem* **2012**, *13*, 3223–3230.
64. Schmidt, R.; Krasselt, C.; von Borczyskowski, C. Change Point Analysis of Matrix Dependent Photoluminescence Intermittency of Single CdSe/ZnS Quantum Dots with Intermediate Intensity Levels. *Chem. Phys.* **2012**, *406*, 9–14.
65. Watkins, L. P.; Yang, H. Detection of Intensity Change Points in Time-Resolved Single Molecule Measurements. *J. Phys. Chem. B* **2005**, *109*, 617–628.
66. Koole, R.; Schapotschnikow, P.; de Mello Donega, C.; Vlugt, T. J. H.; Meijerink, A. Time-Dependent Photoluminescence Spectroscopy as a Tool To Measure the Ligand Exchange Kinetics on a Quantum Dot Surface. *ACS Nano* **2008**, *2*, 1703–1714.
67. Knowles, K. E.; Tice, D. B.; McArthur, E. A.; Solomon, G. C.; Emily, A.; Weiss, E. A. Chemical Control of the Photoluminescence of CdSe Quantum Dot-Organic Complexes with a Series of para-Substituted Aniline Ligands. *J. Am. Chem. Soc.* **2010**, *132*, 1041–1050.
68. Morris-Cohen, A. J.; Vasilenko, V.; Amin, V. A.; Reuter, M. G.; Weiss, E. A. Model for Adsorption of Ligands to Colloidal Quantum Dots with Concentration-Dependent Surface Structure. *ACS Nano* **2012**, *6*, 557–565.
69. Al Salman, A.; Tortschanoff, A.; van der Zwan, G.; van Mourik, F.; Chergui, M. A Model for the Multi-exponential Excited State Decay of CdSe Nanocrystals. *Chem. Phys.* **2009**, *357*, 96–101.
70. Schlegel, G.; Bohnenberger, J.; Potapova, I.; Mews, A. Fluorescence Decay Time of Single Semiconductor Nanocrystals. *Phys. Rev. Lett.* **2002**, *88*, 1374011.
71. Fisher, B. R.; Eisler, H. J.; Stott, N.; Bawendi, M. G. Emission Intensity Dependence and Single-Exponential Behaviour In Single Colloidal Quantum Dot Fluorescence Lifetimes. *J. Phys. Chem. B* **2004**, *108*, 143–148.
72. Biebricher, A.; Sauer, M.; Tinnefeld, P. Radiative and Nonradiative Rate Fluctuations of Single Colloidal Semiconductor Nanocrystals. *J. Phys. Chem. B* **2006**, *110*, 5174–5178.
73. Liptay, T. J.; Marshall, L. F.; Rao, P. S.; Ram, R. J.; Bawendi, M. G. Anomalous Stokes Shift in CdSe Nanocrystals. *Phys. Rev. B* **2007**, *76*, 155314.
74. Dabbousi, B. O.; Redriguez-Vejo, J.; Mikulec, F. V.; Heine, J. R.; Mattousi, H.; Ober, R.; Jensen, K. F.; Bawendi, M. G. (CdSe)ZnS Core–Shell Quantum Dots: Synthesis and Characterization of a Size Series of Highly Luminescent Nanocrystallites. *J. Phys. Chem. B* **1997**, *101*, 9463–9475.
75. Gomez, D. E.; van Emden, J.; Mulvaney, P. Blinking and Surface Chemistry of Single CdSe Nanocrystals. *Small* **2006**, *2*, 204–208.
76. Bullen, C.; Mulvaney, P. The Effects of Chemisorption on the Luminescence of CdSe Quantum Dots. *Langmuir* **2006**, *22*, 3007–3013.

77. Bowen-Katari, J. E.; Colvin, V. L.; Alivisatos, A.P. X-ray Photoelectron Spectroscopy of CdSe Nanocrystals with Application to Studies of the Nanocrystal Surface. *J. Phys. Chem.* **1994**, *98*, 4109–4117.
78. Kilina, S. V.; Neukirch, A. J.; Habenicht, B. F.; Kilin, D. S.; Prezhdo, O. V. Quantum Zeno Effect Rationalizes the Phonon Bottleneck in Semiconductor Quantum Dots. *Phys. Rev. Lett.* **2013**, *110*, 189404.
79. Burda, C.; Green, T. C.; Link, S.; El-Sayed, M. A. Electron Shuttling Across the Interface of CdSe Nanoparticles Monitored by Femtosecond Laser Spectroscopy. *J. Phys. Chem. B* **1999**, *103*, 1783–1788.
80. Jones, M.; Lo, S. S.; Scholes, G. D. Quantitative Modeling of the Role of Surface Traps in CdSe/CdS/ZnS Nanocrystal Photoluminescence Decay Dynamics. *Proc. Natl. Acad. Sci. U.S.A.* **2009**, *106*, 3011–3016.
81. Jones, M.; Lo, S. S.; Scholes, G. D. Signitures of Exciton Dynamics and Carrier Trapping in the Time-Resolved Photoluminescence of Colloidal CdSe Nanocrystals. *J. Phys. Chem. C* **2009**, *113*, 18632–18642.
82. Zenkevich, E. I.; von Borczyskowski, C.; Shulga, A. M. Structure and Excited State Properties of Multiporphyrin Arrays Formed by Supramolecular Design. *J. Porphyrins Phthalocyanines* **2003**, *7*, 731–754.
83. Zenkevich, E. I.; von Borczyskowski, C. Multiporphyrin Self-Assembled Arrays in Solutions and Films: Thermodynamics, Spectroscopy, and Photochemistry. In *Handbook of Polyelectrolytes and Their Applications*; Tripathy, S. K., Kumar, J., Nalwa, H. S., Eds.; American Scientific Publishers: Stevenson Ranch, CA, 2002; Vol. 2, pp 301−348.
84. Murov, S.; Carmichael, I.; Hug, G. *Handbook of Photochemistry*; Marcel Dekker: New York, 1993.
85. Marcus, Y. *Solvent Mixtures*; Marcel Dekker: New York, 2002.
86. Cichos, F.; Willert, A.; Rempel, U.; von Borczyskowski, C. Solvation Dynamics in Mixtures of Polar and Nonpolar Solvents. *J. Phys. Chem. A* **1997**, *101*, 8179–8185.
87. Göhler, C. Fast Spectral Analysis of Blinking Processes in Semiconductor Nanocrystals. Masters Thesis, Chemnitz University of Technology, Chemnitz, 2014.